



Nuutti Vuorimies, Heikki Luomala, Ron Munro and Pauli Kolisoja

STYNIE WOOD DEMONSTRATION PROJECT, MOSSTODLOCH, SCOTLAND

**A Report on a Demonstration of Tyre Pressure Control on Timber Haulage Vehicles
travelling on a Gravel Forest Road**

ABSTRACT

The European Union ROADEX Project 1998 – 2012 was a trans-national roads co-operation that aimed at developing ways for interactive and innovative management of low volume roads across the European Northern Periphery. Its main goals were to facilitate co-operation and research into the common problems of constructing and maintaining low volume roads in harsh climates.

This report gives a summary of a local demonstration of the benefits of the use of tyre pressure control (TPC) on timber haulage vehicles on forest roads in northern Scotland. ROADEX has been a pioneer in the use TPC in the Northern Periphery and the demonstration at Stynie Wood aimed to show the earth pressures that could result from using timber vehicles equipped with TPC, and hence the applicability of the system for forest roads locally.

Four earth pressure cells and one strain gauge were used in the demonstration to measure the passes of two trucks with different wheel types, wheel loadings and tyre pressures. Two lasers were installed on the road shoulder on tripods to measure the drive paths of the wheels. The resulting measured earth pressures and strains have been presented in relation to the drive path of the wheel. Two trucks were used on the test site. The trucks did not have TPC on the steering axle wheels.

The earth pressures measured were mainly as expected. When the earth pressures from the different wheel types were compared with each other it was noticed that the highest earth pressures near to the road surface were caused by with the high tyre pressures on the wheels on the steering axle.

The resilient and permanent parts of the strain measurements were identified separately for each wheel pass. The method used gives some inaccuracies in the calculated values, but has the benefit of presenting all passes alike. The highest permanent strains were measured under the steering axle with a wheel load of 3300 kg, whereas the highest resilient strains were measured under maxi wheels with wheel load about 4200 kg.

The resilient modulus of the upper part of the road was calculated using the measured earth pressures from the topmost earth pressure cell and the resilient strains at between 34 mm and 155 mm deep. The highest calculated resilient modulus on the test site was below 30 MPa.

When drawing conclusions from the demonstration results it should be remembered that the loading sequence of the trucks would also have had an effect on the results which could not be estimated. Despite this uncertainty however, based on the wheel loads and tyre pressures used in the demonstration, it seems that the wheels on the steering axle were the most damaging wheel near to the road surface.

KEYWORDS

CTI, tyre pressure, earth pressure, deformation, resilient strain, drive path, low volume road, forest road, Northern Periphery

PREFACE

This is a final report from Task D2 of the ROADEX “Implementing Accessibility” project, a technical trans-national cooperation project between The Highland Council, Forestry Commission Scotland and the Western Isles Council from Scotland; The Northern Region of The Norwegian Public Roads Administration; The Northern Region of The Swedish Transport Administration and the Swedish Forest Agency; The Centre of Economic Development, Transport and the Environment of Finland; The Government of Greenland; The Icelandic Public Roads Administration; and The National Roads Authority and The Department of Transport of Ireland.

The lead partner of the ROADEX “Implementing Accessibility” project was The Northern Region of The Swedish Transport Administration and the project consultant was Roadscanners Oy from Finland.

This report records a demonstration of the benefits of the use of tyre pressure control (TPC) on timber haulage vehicles on forest roads in northern Scotland. The works includes a GPR survey, installation of instrumentation, testing using two timber haulage vehicles, interpretation and assessment of the measured data, and some conclusions.

The report was compiled by Nuutti Vuorimies and Heikki Luomala under the supervision of Pauli Kolisoja, all from the Laboratory of Earth and Foundations Structures at the Tampere University of Technology (TUT), in collaboration with Ron Munro of Munroconsult Ltd, Scotland. Other persons from the TUT team who were involved in the project include Kauko Sahi, who assisted with the measurement system and Ossi Peltokangas, who pre-processed the raw values from the measured data. Petri Varin from Roadscanners Ltd interpreted the Ground Penetration Radar survey. Mika Pyhähuhta of Laboratorio Uleåborg designed the graphic layout.

The authors would like to express their gratitude to the following persons who made it possible to carry out the demonstration.

Mr Frank MacCulloch, Head of Forestry Civil Engineering
 Alan Drake, Forestry Civil Engineering GPR survey team
 Mr Jim Seaton, Estates and Planning Forester, Moray & Aberdeenshire Forest District
 Mr Jonathan Ritchie, James Jones & Sons Ltd, Mosstodloch

Finally, last but not least, the authors would like to thank the ROADEX IV Project Steering Committee for their guidance and encouragement during the work

Copyright © 2012 The ROADEX “Implementing Accessibility” Project

All rights reserved.

ROADEX “Implementing Accessibility” Lead Partner: The Swedish Transport Administration, Northern Region, Box 809, S-971 25 Luleå. Project co-ordinator: Mr. Krister Palo.

CONTENTS

ABSTRACT.....	2
PREFACE.....	3
CONTENTS.....	4
1. INTRODUCTION	6
1.1. THE ROADEX PROJECT	6
1.2. TASK D2 ROAD FRIENDLY VEHICLES & TYRE PRESSURE CONTROL.....	7
2. GENERAL DESCRIPTION OF THE ROAD	8
2.1. LOCATION	8
2.2. TRAFFIC VOLUME AND TYPE OF TRAFFIC/IMPORTANCE OF THE ROAD.....	8
2.3. TYPE OF ROAD STRUCTURE	9
2.4. LANDSCAPE AND TERRAIN	10
2.5. GROUND CONDITIONS ON A GENERAL LEVEL	11
2.6. TYPICAL PROBLEMS OF THE ROAD.....	11
3. SYSTEM OF MEASUREMENT	12
3.1. TRANSDUCERS	12
3.1.1. Earth pressure gauges	12
3.1.2. Strain gauge	12
3.1.3. Laser measurement and video camera for measuring the driving path.....	13
3.2. LEVELLING	14
3.3. LOCATION OF THE GAUGES	14
4. TIMBER TRUCKS WITH TYRE PRESSURE CONTROL.....	15
4.1. TRUCK 1	15
4.1.1. Wheels of Truck 1	15
4.1.2. Loadings of Truck 1	15
4.1.3. Tyre pressures and contact area of wheels	15
4.2. TRUCK 2	17
4.2.1. Wheels of Truck 2	17
4.2.2. Loadings of Truck 2	17
4.2.3. Tyre pressures and contact pressures of wheels.....	17
5. DRIVING SEQUENCES AND WEATHER	18

5.1. DRIVING DIRECTIONS, LOADS AND WHEEL PRESSURES AND GRADING OF THE ROAD	18
5.1.1. Truck 1.....	18
5.1.2. Truck 2.....	19
5.2. WEATHER DURING MEASUREMENTS.....	19
6. RESULTS OF MEASUREMENTS.....	20
6.1. EARTH PRESSURE MEASUREMENTS	20
6.1.1. Truck 1.....	20
6.1.2. Truck 2.....	25
6.1.3. Difference between wheel types and the trucks.....	27
6.2. STRAIN GAUGE MEASUREMENTS.....	30
6.3. RUTTING AND DEFORMATIONS ON THE ROAD SURFACE	40
7. ANALYSIS OF THE MEASUREMENTS	41
7.1. MODULUS.....	41
8. SUMMARY	44

1. INTRODUCTION

1.1. THE ROADEX PROJECT

The ROADEX Project is a technical co-operation between road organisations across northern Europe that aims to share road related information and research between the partners. The project was started in 1998 as a 3 year pilot co-operation between the districts of Finland Lapland, Troms County of Norway, the Northern Region of Sweden and The Highland Council of Scotland and was subsequently followed and extended with a second project, ROADEX II, from 2002 to 2005, a third, ROADEX III from 2006 to 2007 and a fourth, ROADEX “Implementing Accessibility” from 2009 to 2012.



Figure 1.1 *The Northern Periphery Area and ROADEX Partners*

The Partners in the ROADEX “Implementing Accessibility” project comprised public road administrations and forestry organisations from across the European Northern Periphery. These were The Highland Council, Forestry Commission Scotland and the Western Isles Council from Scotland, The Northern Region of The Norwegian Public Roads Administration, The Northern Region of The Swedish Transport Administration and the Swedish Forest Agency, The Centre of Economic Development, Transport and the Environment of Finland, The Government of Greenland, The Icelandic Public Road Administration and The National Roads Authority and The Department of Transport of Ireland.

The aim of the project was to implement the road technologies developed by ROADEX on to the partner road networks to improve operational efficiency and save money. The lead partner for the project was The Swedish Transport Administration and the main project consultant was Roadscanners Oy of Finland.

The project was awarded NPP funding in September 2009 and held its first steering Committee meeting in Luleå, November 2009.

A main part of the project was a programme of 23 demonstration projects showcasing the ROADEX methods in the Local Partner areas supported by a new pan-regional “ROADEX Consultancy Service” and “Knowledge Centre”. Three research tasks were also pursued as part of the project: D1 “Climate change and its consequences on the maintenance of low volume roads”,

D2 “Road friendly vehicles & tyre pressure control” and D3 “Vibration in vehicles and humans due to road condition”. All of the reports are available on the ROADDEX website at www.roadex.org.

1.2. TASK D2 ROAD FRIENDLY VEHICLES & TYRE PRESSURE CONTROL

ROADDEX has been a pioneer in the use of ‘road friendly’ timber haulage vehicles and tyre pressure control (TPC) across the Northern Periphery. These technologies did not exist in Scotland or Finland before being introduced in ROADDEX III and now numbers are growing in response to changing economic conditions and environmental considerations. This is particularly the case for weak public rural roads where public road organisations and forest agencies are coming under pressure to permit haulage along weak roads to support local communities. The ROADDEX D2 demonstration projects aimed to demonstrate the operational, commercial & environmental benefits that can be gained in the use of road friendly vehicles on weak roads.

The testing at Stynie Wood, Mosstodloch in northern Scotland was the Scottish demonstration of the benefits of the use of TPC on a low volume forest road. It aimed to demonstrate the ground pressures that could result when using timber vehicles equipped with a system of TPC and hence the applicability of the system for weak forest roads. The demonstration was carried out on a minor forest road in the Stynie Wood, close to Mosstodloch, Morayshire. The location of the demonstration was chosen in conjunction with the Forestry Commission and James Jones & Sons Ltd as the most suitable location for trucks and testing. The two timber haulage vehicles in the test were supplied by James Jones & Sons Ltd, and their input is gratefully acknowledged.

2. GENERAL DESCRIPTION OF THE ROAD

2.1. LOCATION

Stynie Wood forest road is located in the Moray & Aberdeenshire Forest District of the Forestry Commission (Scotland), just north of the village of Mosstodloch in north east Scotland, close to the sawmills of James Jones & Sons Ltd as shown in Figure 2.1.

The location of the test road was chosen due to its proximity to the James Jones & Sons Ltd sawmill and the availability of timber haulage vehicles using the premises.

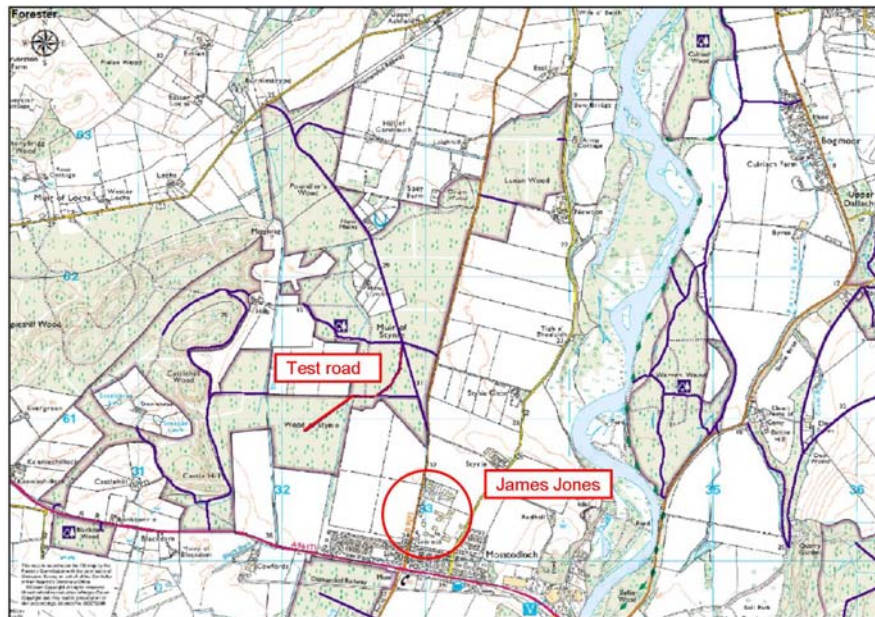


Figure 2.1 Location of the test road relative to the James Jones & Sons Ltd sawmill, Mosstodloch

2.2. TRAFFIC VOLUME AND TYPE OF TRAFFIC/IMPORTANCE OF THE ROAD

The test road had been classified as a Class B forest “spur road” at the time and was only being used a temporary stockpiling location of logs to supply the local sawmill as Figure 2.2 shows. The Class B road classification was subject to annual review according to need as below:

Class B – spur roads:

- Used by timber haulage lorries for specific operations.
- Full geometric and safety standards.
- Specification tailored to suit purpose.
- Possibility that surfacing not high quality or durable.
- Long term maintenance minimal.
- Each usage subject to individual engineering assessment.
- Limiting features noted for each particular contract.

Class B was part of a 4 class forest road hierarchy of

1. Class A - main roads
2. Class B - spur roads
3. Class C - other roads
4. Unclassified roads



Figure 2.2 Temporary stockpiles of logs on the Class B test road

2.3. TYPE OF ROAD STRUCTURE

The test road section comprised a gravel road with a running width of between 3.0m and 3.4m along the test road section. Narrow grassy shoulders were available outwith the running surface that could be used for trafficking in an emergency. A turning facility had been constructed at the end of the section suitable for turning large timber vehicles. Figure 2.3 shows the small test pit made at the distance 741.5m.

The road construction typically comprised:

- 0-0.20m, a sandy gravel with cobbles <75mm
- 0.20-0.35m dark brown sandy gravel with cobbles<50mm
- 0.35m root fragments
- 0.35-0.40m brown silty sand



Figure 2.3 The small test pit from the middle line of the test road at distance 741.5m.

A Ground Penetrating Radar (GPR) survey was carried out by the Forestry Commission in-house GPR survey team and analysed by Roadscanners Oy. Measurements were made in one direction during September 2010 and the analysis was done following the tests on site. The resulting GPR interpretations between chainages 700-800 are shown in Figure 2.4. The base course of the test section was little less than 0.20m and the depth of the road structure was mainly 0.40m.

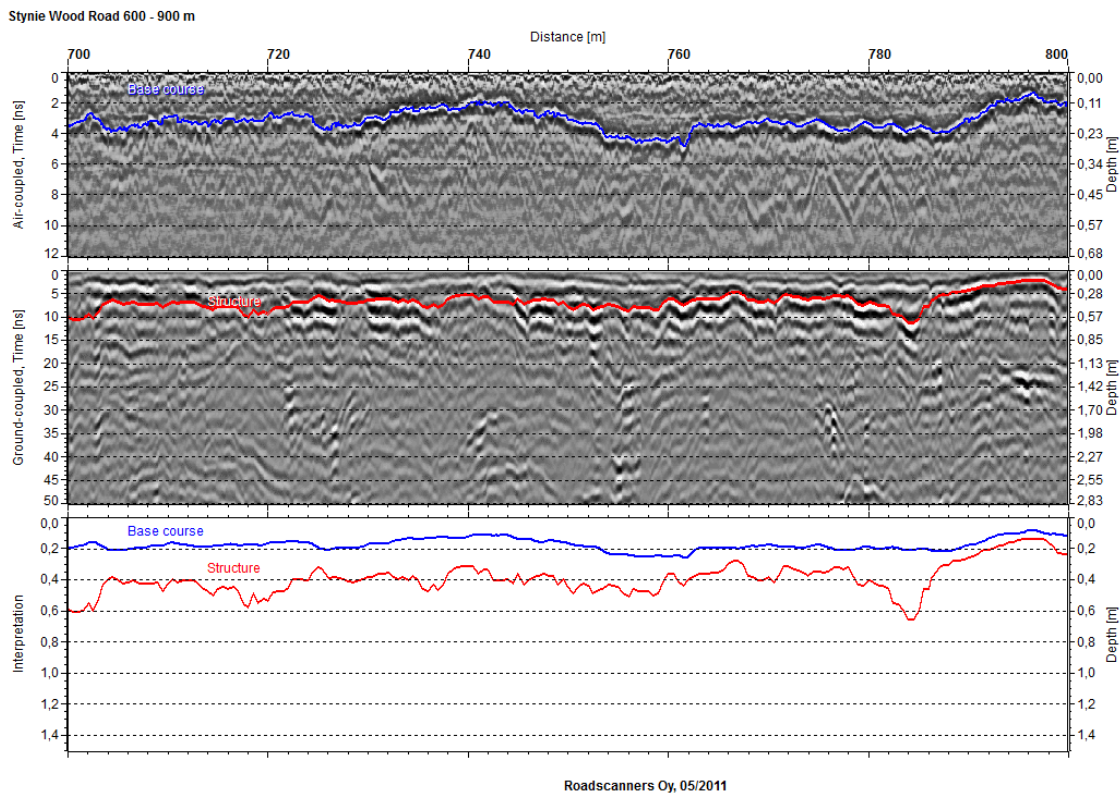


Figure 2.4. Ground Penetrating Radar interpretations of the test site.

2.4. LANDSCAPE AND TERRAIN

The landscape at the demonstration site was generally flat and gently undulating with mature forest on both sides. Figure 2.5 shows the test section looking toward the turning facility.



Figure 2.5 The test section looking toward the turning facility

2.5. GROUND CONDITIONS ON A GENERAL LEVEL

The ground conditions were typical of a former raised beach formation, ie dry silty sandy gravel conditions with a thin organic layer capable of sustaining trees.

2.6. TYPICAL PROBLEMS OF THE ROAD

There were no problems evident on the road on the days of the survey, but the road had not been used for heavy timber haulage in the immediate past. The road surface was dry and well compacted with a narrow, but acceptable, shape.

3. SYSTEM OF MEASUREMENT

3.1. TRANSDUCERS

3.1.1. Earth pressure gauges

The vertical pressure in the road was measured by earth pressure gauges at different depths. The gauges used were strain gauge soil pressure transducers with a maximum pressure range of 500 kPa and 1000 kPa. The two lower range gauges were installed deeper in the road and the higher range sensors closer to the surface where the earth pressures were higher. The deepest earth pressure gauge was installed first in the road. Figure 3.1 shows the gauge as installed before backfilling. Levelling sand was used below the gauges where necessary. The next gauge was installed approximately 10 cm higher and a slightly forward so that the gauges did not affect each other, and compaction around the gauges could be done efficiently using as much original material from the road layer as possible. The material around the gauges was first compacted by hand as hard as possible and compaction was thereafter finished by the hand rammer shown in Figure 3.1. Pressure measurement was the key aim of the test.



Figures 3.1 The earth pressure gauge at the deepest installing level and the hand rammer used

3.1.2. Strain gauge

One strain gauge was installed in the middle of the earth pressure gauges. The idea for using the strain gauge was to try to get usable information on the deformations in the layer. Figure 3.2 shows the strain gauge used. The transducer was based on a linear variable displacement transducer (LVDT) and measured the distance between the two plates. The measurement range between plates was 100-130 mm and the practical accuracy was 1/1000 of the 30 mm measurement range. The foot of the sensor was installed into a drilled hole without the upper plate. The layer to be monitored was placed and compacted, at which point the upper plate was attached to the measurement bar.

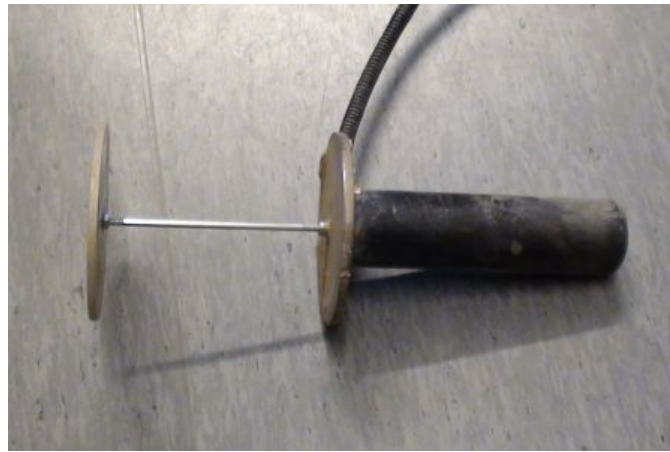


Figure 3.2 The strain gauge

3.1.3. Laser measurement and video camera for measuring the driving path

It was known that the drive path of the vehicle would have an effect on the planned measurements and it was decided that the path of the truck would be measured using lasers. A laser measures the distance to an object within a range of 0.2 to 10 metres. Two lasers were installed on the road shoulder on tripods. The lasers were about 2m from the earth pressure gauges. The distance from earth pressure gauge line was measured by measuring tape and the accuracies of the lasers were checked in the working range. The distance between the lasers was approximately 1.3m. The laser was used to measure the drive path as shown in Figure 3.3.

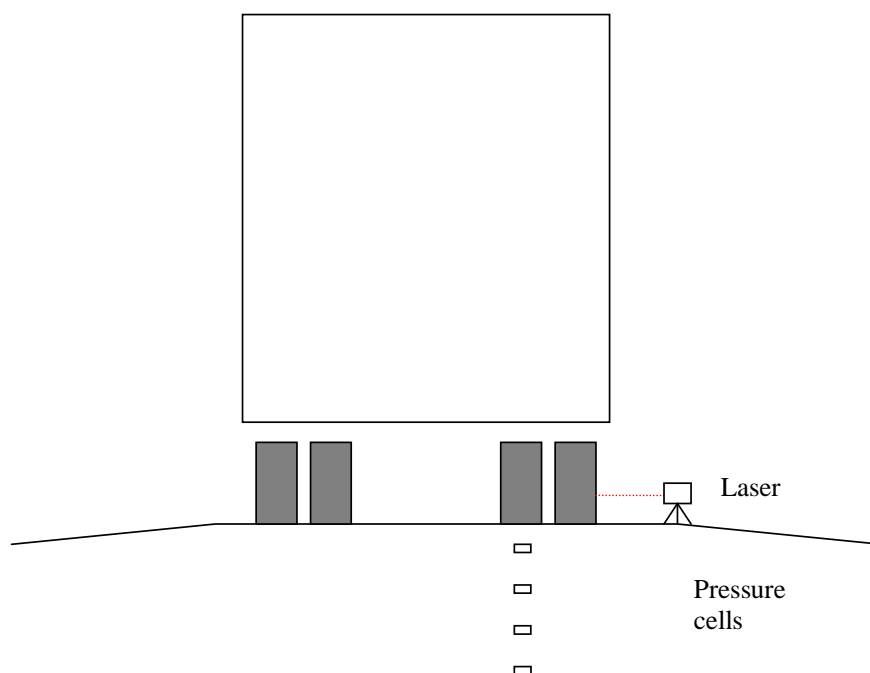


Figure 3.3 Schematic instrumentation plan in Stynie Wood

Each pass of the test vehicle was recorded on video tape as a permanent record of the test. A grid was painted on the road surface on the driving line. Each square was 50mm by 50mm. Figure 3.4 shows the painted grid, the driving guidance line and the cables leading from the installed gauges. The grid and the lines had to be repainted occasionally. The line assisted the truck driver to change the driving line on each pass.



Figure 3.4 The painted grid and guidance line for driving in Stynie Wood

3.2. LEVELLING

The level of each gauge was measured using an engineer's level and referenced back to fixed hard reference points on each side of the road. The road level above the gauges was also measured before the commencement of passes. The road level measurements were repeated during the tests usually after each passing series. The levels of the gauges were measured again at the end of the testing programme when the gauges were removed.

3.3. LOCATION OF THE GAUGES

The gauges were situated between chainage 743.5m and 744.9m on the right wheel path. The top of the earth pressure gauges varied from 67mm to 389mm as measured from the road surface at the beginning of the tests. Earth pressure gauge P1 was the nearest to the surface of the road and P4 was the deepest earth pressure gauge. The strain gauge (SG) was set to measure deformation between 34mm and 158mm. Figure 3.5 illustrates the locations of the gauges at the beginning of the testing.

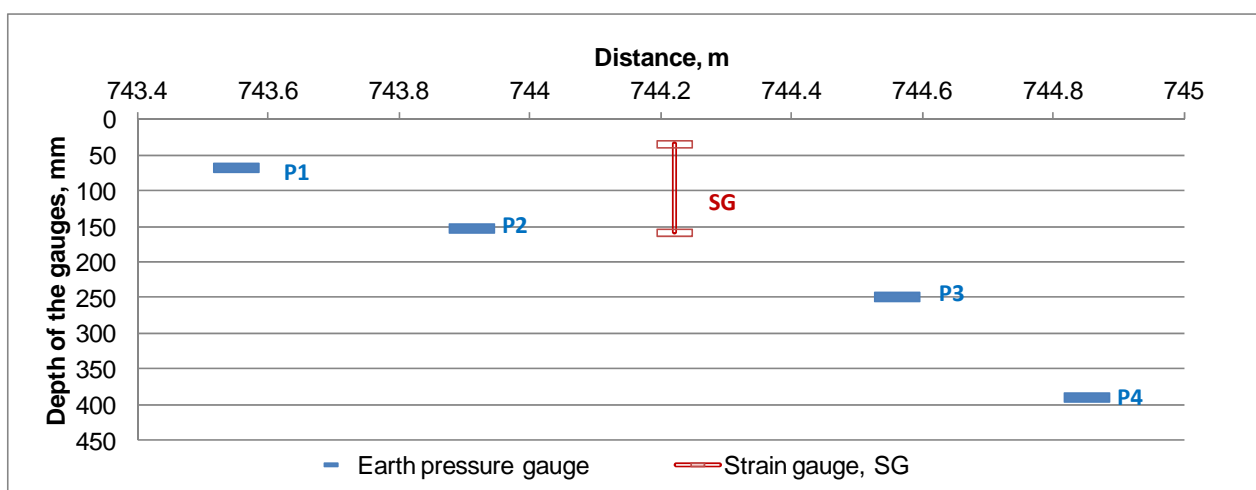


Figure 3.5 Locations of the gauges at the beginning of the test in Stynie Wood

4. TIMBER TRUCKS WITH TYRE PRESSURE CONTROL

Two timber trucks, “Truck 1” and “Truck 2”, were used in the demonstration task. Both were equipped with a system of tyre pressure control, also generically known as “central tyre inflation”, or CTI. Detailed descriptions of the wheel and tyre configurations of each truck are set out in the following sections.

4.1. TRUCK 1

4.1.1. Wheels of Truck 1

Truck 1 had six axles. The steering tyres (315/80 R 22.5) were not equipped with CTI. The second axle was the driving axle. This had twin tyres (315/80 R 22.5). On the same bogey as the driving wheels was the third axle which had single tyres (315/80 R 22.5). The third axle was lifted up when the truck was not loaded. The trailer had three axles with maxi tyres (455/45 R22.5).

4.1.2. Loadings of Truck 1

Truck 1 was weighed loaded and unloaded after the measurements. The measurements were carried out on an even asphalt area in the adjacent sawmill of James Jones & Sons Ltd. Each axle was weighed separately with weigh pads under each wheel so that the wheel loads could be determined. According to these measurements the total weight of Truck 1 without load was 20,820 kg. The empty truck weighed 14,460 kg and the empty trailer 6,360 kg. The loaded Truck 1 weighed 44,120 kg, of which the truck weighed 19,620 kg and the trailer 24,500 kg. Table 4.1 shows the measured wheel loads and axle loads of Truck 1. Interestingly the driving axle of the empty truck weighed 1000 kg more than the same axle of the loaded truck as the third axle was lifted up in the empty truck.

Table 4.1. The wheel and axle loads of the truck 1.

axle and wheel type	Truck 1 without timber load			Truck 1 with the timber load		
	left side	right side	axle load	left side	right side	axle load
1.single	2620	2740	5360 kg	3180	3360	6540 kg
2.twin	4820	4280	9100 kg	4080	4000	8080 kg
3.single	Up	Up	Up	2660	2340	5000 kg
4.maxi	1100	860	1960 kg	4260	3760	8020 kg
5.maxi	1060	1060	2120 kg	4280	3880	8160 kg
6.maxi	840	1440	2280 kg	4040	4280	8320 kg

4.1.3. Tyre pressures and contact area of wheels

Two different tyre pressure settings were used with the empty Truck 1 during the test measurements. Four different tyre pressure settings were used with the loaded timber Truck 1. The contact areas of the wheels with different tyre pressures were measured at the same time that the wheel loads of were weighed. This was done using a large scale vernier caliper assuming the contact area being rectangular (Figure 4.1). When the area of a twin tyre was measured only the outer wheel was measured and it was assumed that the inner wheel was similar to the outer wheel.

The contact pressure of a wheel was calculated by dividing the weight of the wheel by the measured contact area. Table 4.2 shows the tyre pressures and calculated contact pressures for the wheels of empty Truck 1. Table 4.3 shows the tyre pressures and calculated contact pressures for the wheels of Truck 1 loaded with timber.



Figure 4.1 Measuring the contact area of a wheel using the vernier caliper.

Table 4.2. Tyre pressures and calculated contact pressures for the wheels of empty Truck 1.

wheel type	Single	twin	twin	maxi	maxi	Maxi
high pressure; kPa	814	690	690	897	897	897
contact pressure, right	418 kPa	300 kPa	up	123 kPa	236 kPa	245 kPa
contact pressure, left	492 kPa	321 kPa	up	194 kPa	210 kPa	185 kPa
low pressure; kPa	814	414	414	414	414	414
contact pressure, right	418 kPa	291 kPa	up	120 kPa	236 kPa	243 kPa
contact pressure, left	492 kPa	305 kPa	up	210 kPa	209 kPa	185 kPa

Table 4.3. Tyre pressures and calculated contact pressures for the wheels of Truck 1 loaded with timber.

wheel type	Single	twin	single	maxi	maxi	Maxi
high pressure; kPa	814	690	690	897	897	897
contact pressure, right	445 kPa	294 kPa	465 kPa	476 kPa	434 kPa	507 kPa
contact pressure, left	497 kPa	331 kPa	435 kPa	550 kPa	537 kPa	480 kPa
quite high pressure; kPa	814	586	586	690	690	690
contact pressure, right	445 kPa	290 kPa	386 kPa	426 kPa	407 kPa	474 kPa
contact pressure, left	497 kPa	326 kPa	417 kPa	512 kPa	506 kPa	462 kPa
quite low pressure; kPa	814	517	517	586	586	586
contact pressure, right	445 kPa	282 kPa	386 kPa	383 kPa	395 kPa	452 kPa
contact pressure, left	497 kPa	307 kPa	389 kPa	449 kPa	476 kPa	443 kPa
low pressure; kPa	814	317	317	469	469	469
contact pressure, right	456 kPa	231 kPa	289 kPa	342 kPa	347 kPa	401 kPa
contact pressure, left	501 kPa	255 kPa	304 kPa	413 kPa	399 kPa	395 kPa

4.2. TRUCK 2

4.2.1. Wheels of Truck 2

Truck 2 had six axles. The steering tyres (315/80 R 22.5) did not have CTI. The second and third axles had driving wheels on the same bogey. The driving wheels had twin tyres (295/80 R22.5). The trailer had three axles of super single tyres (385/65 R22.5).

4.2.2. Loadings of Truck 2

Truck 2 was weighed with its timber load after the ground pressure measurements. The measurements were carried out on an even asphalt area in the adjacent sawmill of James Jones & Sons Ltd. Each axle was weighed separately with weigh pads under each wheel so that the wheel loads could be determined. According to these measurements the total weight of Truck 2 with loaded with timber was 45,840 kg, of which the truck weighed 21,860 kg and the trailer 23,980 kg. Table 4.4 shows the measured wheel loads and axle loads of the Truck 2 loaded with timber.

Table 4.4. Wheel and axle loads of Truck 2.

axle and wheel type	Truck 2 with the timber load		
	left side	right side	axle load
1. single	2840	2780	5620 kg
2. twin	4160	4360	8520 kg
3. twin	4200	3520	7720 kg
4. super single	4180	3640	7820 kg
5. super single	4240	3740	7980 kg
6. super single	4180	4000	8180 kg

4.2.3. Tyre pressures and contact pressures of wheels

Two different tyre pressure settings were used with the loaded Truck 2 during the test measurements and the truck was weighed and measured in a similar way to Truck 1. When the area of a twin tyre was measured only the outer wheel was measured and it was assumed that the inner wheel was similar to the outer wheel.

The contact pressure of the wheels was calculated by dividing the weight of the wheel by the measured contact area. Table 4.5 shows the tyre pressures and calculated contact pressures of the wheels for Truck 2 loaded with timber.

Table 4.5. Tyre pressures and calculated contact pressures for the wheels of timber loaded Truck 2.

Wheel type	single	twin	twin	super s	super s	super s
quite high pressure; kPa	690	483	483	690	690	690
contact pressure, right	417 kPa	306 kPa	259 kPa	412 kPa	406 kPa	421 kPa
contact pressure, left	445 kPa	318 kPa	326 kPa	483 kPa	461 kPa	467 kPa
low pressure; kPa	690	317	317	448	448	448
contact pressure, right	417 kPa	287 kPa	239 kPa	405 kPa	375 kPa	391 kPa
contact pressure, left	445 kPa	279 kPa	269 kPa	413 kPa	415 kPa	413 kPa

5. DRIVING SEQUENCES AND WEATHER

5.1. DRIVING DIRECTIONS, LOADS AND WHEEL PRESSURES AND GRADING OF THE ROAD

5.1.1. Truck 1

Truck 1 was used from 13:00 to 16:10. Table 5.1 shows the truck passing times and loadings, the number of passes and the tyre pressure setting. Normally Truck 1 reversed back after passing over the gauges, but twice the truck continued on to a turning place and the loading side of the truck 1 was changing. After the tests an attempt was made to level out the rutting that had developed by reversing the trailer of Truck 1 over the measurement section.

Table 5.1 Passing series for Truck 1

Time	Load	Tyre pressure	Amount	Wheel side
13:25 – 13:35	Empty	Low	11	R
13:35 – 13:45	Empty	Low	9	L
13:55 – 14:05	Empty	Full	9	L
14:30 - 14:40	Full	Low	12	R
14:45 - 14:55	Full	Quite low	10	R
15:20 – 15:30	Full	Quite high	8	R
15:35 – 15:45	Full	High	4	R
15:55 – 16:10	Full	Low	6	R

The road had begun to rut by the time the fully loaded truck passed over the measuring area. Some gravel and sand was added into the rut on the measuring area at 15:00 hrs. Figure 5.1 shows the situation before the material was added, when the rut depth was over 30mm. The road level was measured before and after the addition of material. After this the level of the road was measured after each passing series.



Figure 5.1 Photographs of the rutting developed after 22 passes of loaded Truck 1 at 15:00 hrs.

5.1.2. Truck 2

Truck 2 was used from 17:10 to 18:05. Truck 2 always turned at the turning places so that every pass measured a different side of the truck. As the measurements with Truck 2 were reaching an end it was noticed that the road was becoming more easily damaged and that the rutting was guiding the truck to the same path for every pass. Figures 5.2 and 5.3 show the development of rutting after testing with low tyre pressures of Truck 2 and at the end of the testing. Figure 5.3 shows that the surface of the road was becoming plastic. The edges of the ruts are much sharper as a result of the increasing tyre pressures.

Table 5.2. Passing series for Truck 2.

Time	Load	Tyre pressure	Amount	Wheel side
17:20 – 17:50	Full	Low	6	R & L
18:00 – 18:15	Full	Quite high	9	R & L



Figure 5.2 Rutting developed after Truck 1 passes and 6 passes of loaded Truck 2.



Figure 5.3 Rutting at the end of testing.

5.2. WEATHER DURING MEASUREMENTS

The weather was mostly good for the period of the tests. There was some moisture in the air but the sun was shining. The temperatures were around 15 °C.

6. RESULTS OF MEASUREMENTS

6.1. EARTH PRESSURE MEASUREMENTS

6.1.1. Truck 1

6.1.1.1. Steering axle wheel

The tyres on the steering axle were not connected to the CTI system and were held constant at 814 kPa throughout the test. Figure 6.1 shows the measured earth pressures in the pressure gauges due to the steering axle wheel of loaded Truck 1. The maximum level for each earth pressure gauge is indicated by a horizontal coloured line and numerical value. As a comparison, the comparable earth pressures from the steering axle wheel of empty Truck 1 are shown in Figure 6.2.

The differences in the earth pressures measured arise directly from the wheel loads of the empty and loaded Truck 1 except for the pressures in earth pressure gauge P1. Interestingly, the measured pressures near the road surface are fairly close between the empty and loaded Truck 1. The maximum earth pressures can be seen to be on a narrow drive path, as was intended. However it seems that the width of drive path from the empty Truck 1 is narrower than that of the loaded Truck 1. A reason for this could be that the loading from the steering axle wheel of the empty truck was more concentrated due to the high tyre pressure compared to the loadings from the loaded truck. This would result in comparatively high earth pressures from the empty truck near the road surface. This effect vanished by the depth of the earth pressure gauge P2.

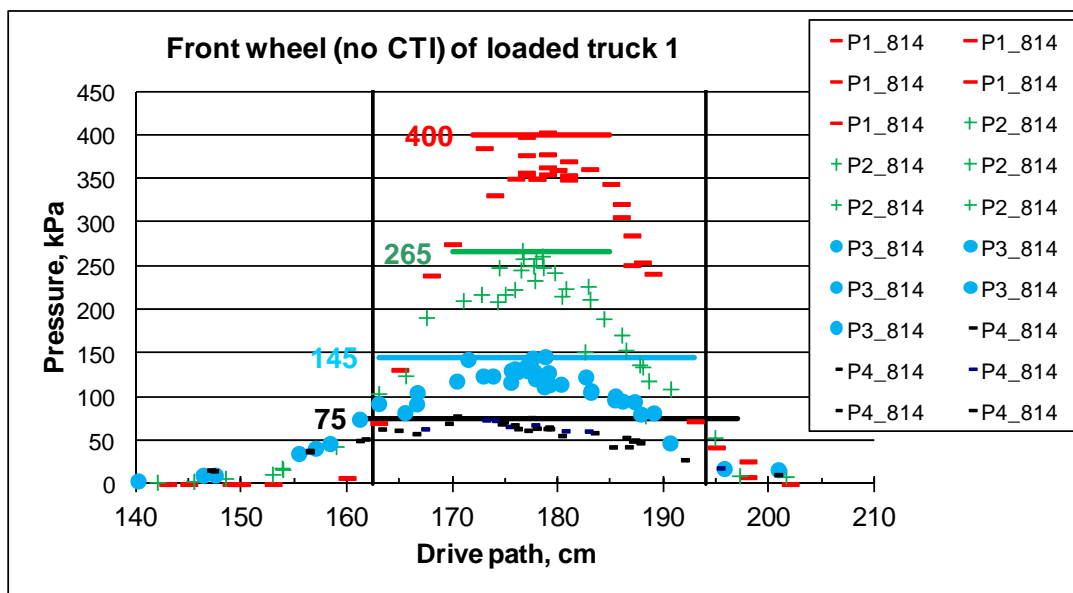


Figure 6.1 Earth pressures resulting from the steering axle wheel of loaded Truck 1 at different depths. “Drive path” means the distance from the lasers. The depths of the earth pressure cell were 67 (P1), 152 (P2), 248 (P3) and 389 mm (P4).

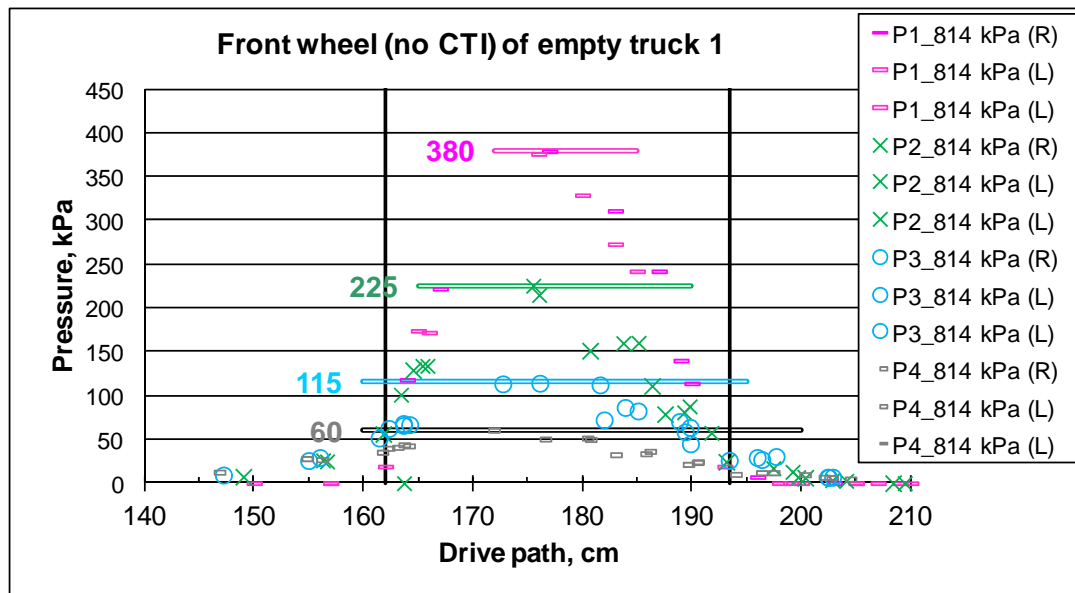


Figure 6.2 Earth pressures resulting from the steering axle wheel of loaded Truck 1 at different depths. “Drive path” means the distance from the lasers. Depths of the earth pressure cell were 67 (P1), 152 (P2), 248 (P3) and 389 mm (P4).

6.1.1.2. Driving wheel

Truck 1 had only one driving axle with twin wheels. Figure 6.3 shows the measured earth pressures at different depths due to the driving wheel of the loaded truck. Figures 6.4 and 6.5 give the measured earth pressures due to the passage of the empty truck. When Truck 1 was empty the third axle was lifted up, with the result that the drive axle load was 1000 kg higher in the empty truck than in the loaded truck. When the wheel load of the empty truck was measured it was noticed that the weight on the left side (4820 kg) was substantially higher than the right (4280 kg). Therefore the loadings from the left side and the right side wheels are produced as separate figures.

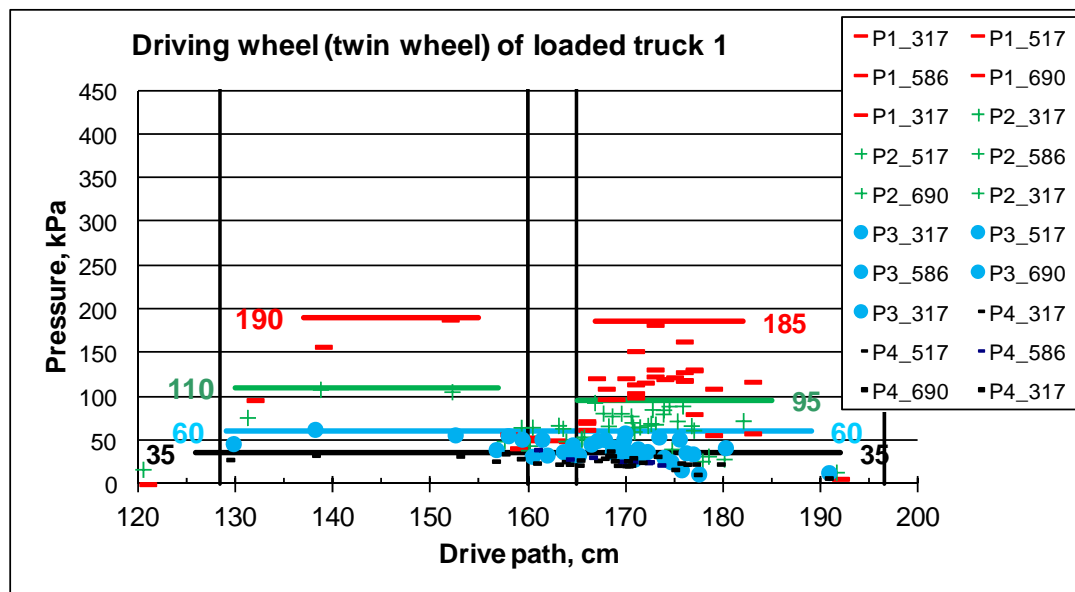


Figure 6.3 Earth pressures resulting from the driving wheel of loaded Truck 1 at different depths. “Drive path” means the distance from the lasers. The depths of the earth pressure cell were 67 (P1), 152 (P2), 248 (P3) and 389 mm (P4).

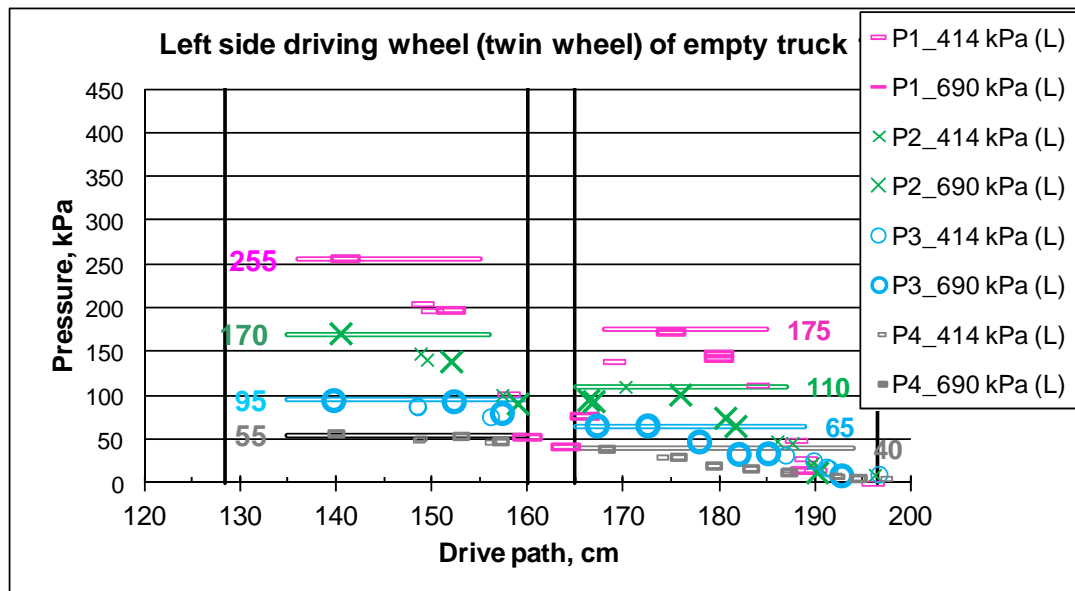


Figure 6.4 Earth pressures resulting from the left side driving wheel of empty Truck 1 at different depths. “Drive path” means the distance from the lasers. Tick marks mean higher tyre pressure. The depths of the earth pressure cell were 67 (P1), 152 (P2), 248 (P3) and 389 mm (P4).

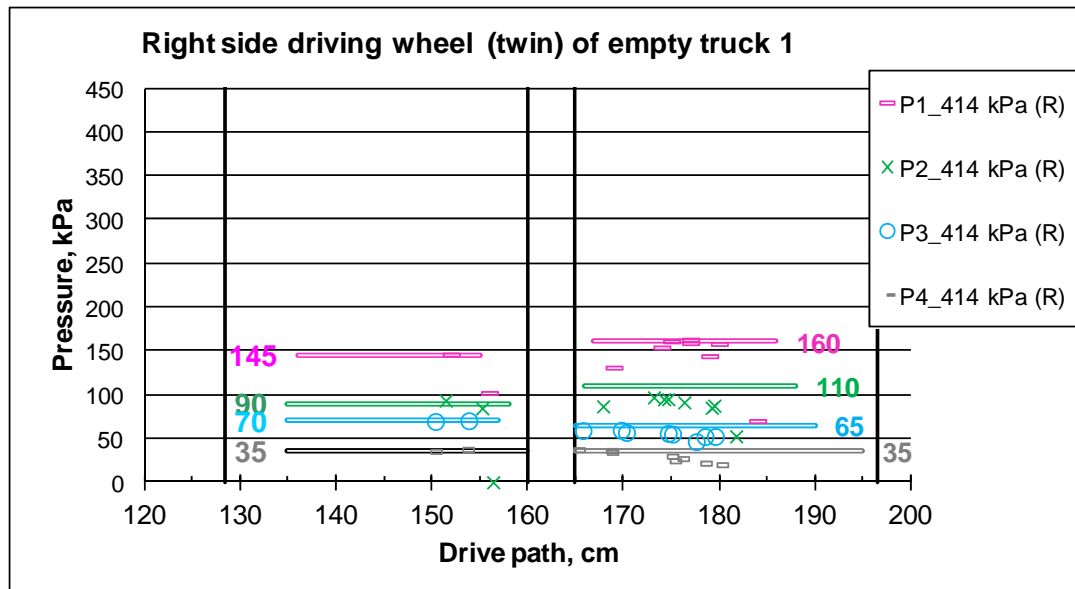


Figure 6.5 Earth pressures resulting from the right side driving wheel of empty Truck 1 at different depths. “Drive path” means the distance from the lasers. The depths of the earth pressure cell were 67 (P1), 152 (P2), 248 (P3) and 389 mm (P4).

Comparing the effects of the different tyre pressures in the twin wheels was not conclusive. The main reason for this is illustrated in figure 6.6. The driving path during the test was narrow resulting in rutting developing. This caused the inner part of the twin wheel assembly to run on the crown of the road and the wheel load to vary depending on how much the inner wheel contacted the crown. When the wheel drove closer to the laser the wheel load spread more evenly on the road surface and higher earth pressures were measured. Unfortunately not enough passes were made on the various driving lines to form any reliable conclusions on the effect of changing tyre pressures in twin wheels.

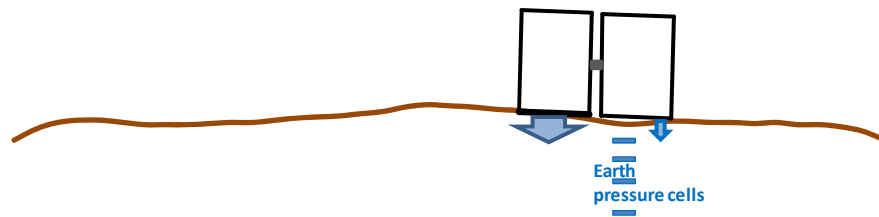


Figure 6.6 Twin wheels on a narrow forest road.

6.1.1.3. Single wheel of the third axle

Figure 6.7 shows the measured earth pressures under the wheel of the third axle of loaded Truck 1. The sequence of truck tyre pressures was low, quite low, quite high, high and low again. The “quite high” and “high” tyre pressures are presented in the same graphic as the pressures were quite near each other and there were only four truck passes with high tyre pressure. These passes were also made after adding aggregate to the ruts on the surface of the road. Earth pressure changes were clearly noticeable on the two topmost earth pressures as the tyre pressure changed, but below 250 mm the difference between the measured pressures were quite small.

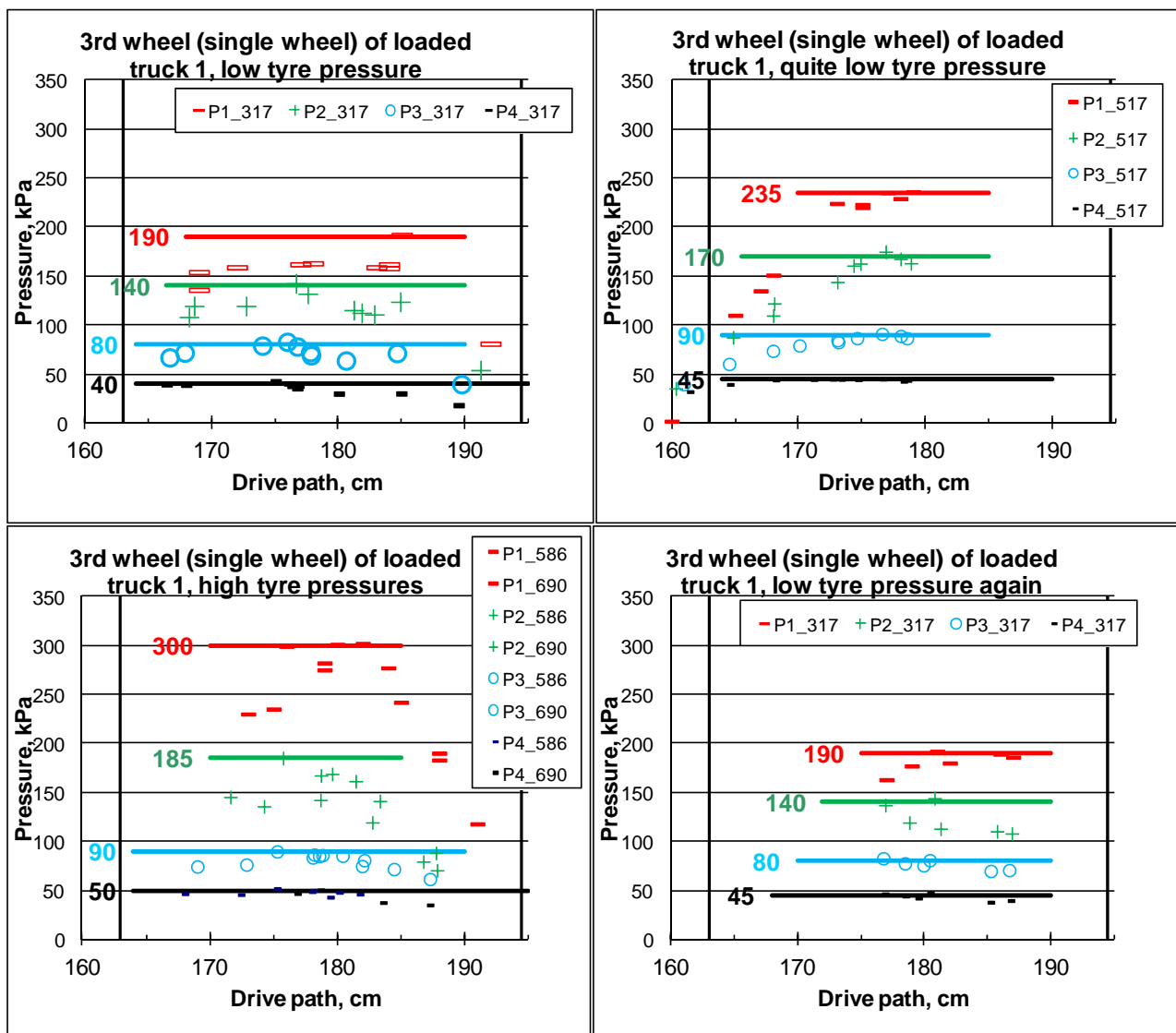


Figure 6.7 Earth pressures resulting from the third wheel (single wheel) of loaded Truck 1 at different depths. The four diagrams are in the same sequence as the truck passes. “Drive path” means the distance from the lasers.

6.1.1.4. Maxi wheels of trailer

As the trailer of Truck 1 had three axles of maxi wheels, a lot of data was recovered from a single truck pass. Figure 6.8 shows the measured earth pressures in P1 for the maxi wheels with low tyre pressure on the right side of the empty truck. The difference in the wheel loads in the three trailer tyres can be seen in the differences of the measured earth pressures. Figure 6.9 similarly shows effect on the measured earth pressure when the wheel load was changed from 1100 kg to 840 kg. Figure 6.10 shows that the earth pressures at depth 152 mm were about half of the values at depth 67 mm. As the depth increased the effect of the wheel load or tyre pressure on the earth pressures could not be measured. Measured earth pressures were 30-40 kPa at the depth of 248 mm and 15-20 kPa at the depth of 389 mm.

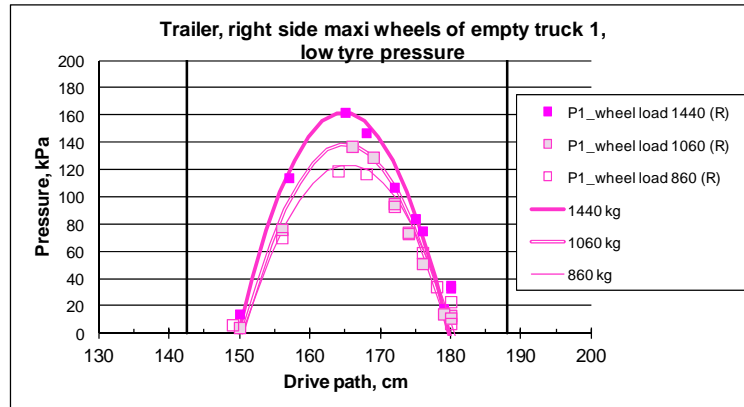


Figure 6.8 Earth pressures near the road surface (depth 67 mm) resulting from the maxi wheels of empty Truck 1 with low tyre pressure. “Drive path” means the distance from the lasers.

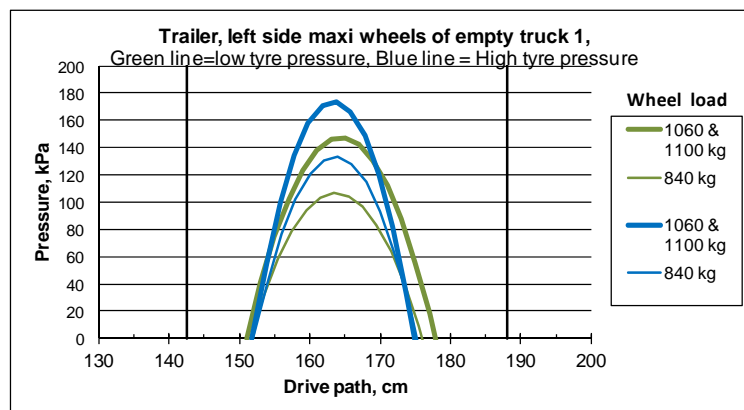


Figure 6.9 Earth pressures near the road surface (depth 67 mm) resulting from the maxi wheels of empty Truck 1 with low and high tyre pressures. “Drive path” means the distance from the lasers.

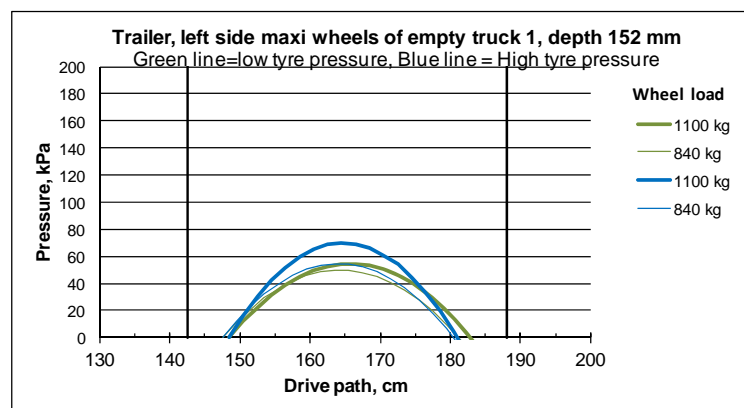


Figure 6.10 Earth pressures at depth 152 mm resulting from the maxi wheels of empty Truck 1 with low and high tyre pressures. “Drive path” means the distance from the lasers.

Figure 6.11 shows the measured earth pressures under the tyre of the third axle of loaded Truck 1. The sequence of tyre pressures was low, quite low, quite high, high and low again. The “quite high” and “high” tyre pressures are presented in the same graphic as the pressures were quite near each other and there were only four truck passes with high tyre pressure. These passes were also made after adding aggregate to the ruts on the surface of the road. Earth pressure changes were clearly noticeable on the two topmost earth pressures as the tyre pressure changed, but below 150 mm the difference between the measured pressures were quite small. The measured earth pressures below 5th and 6th axles were very similar to the 4th axle.

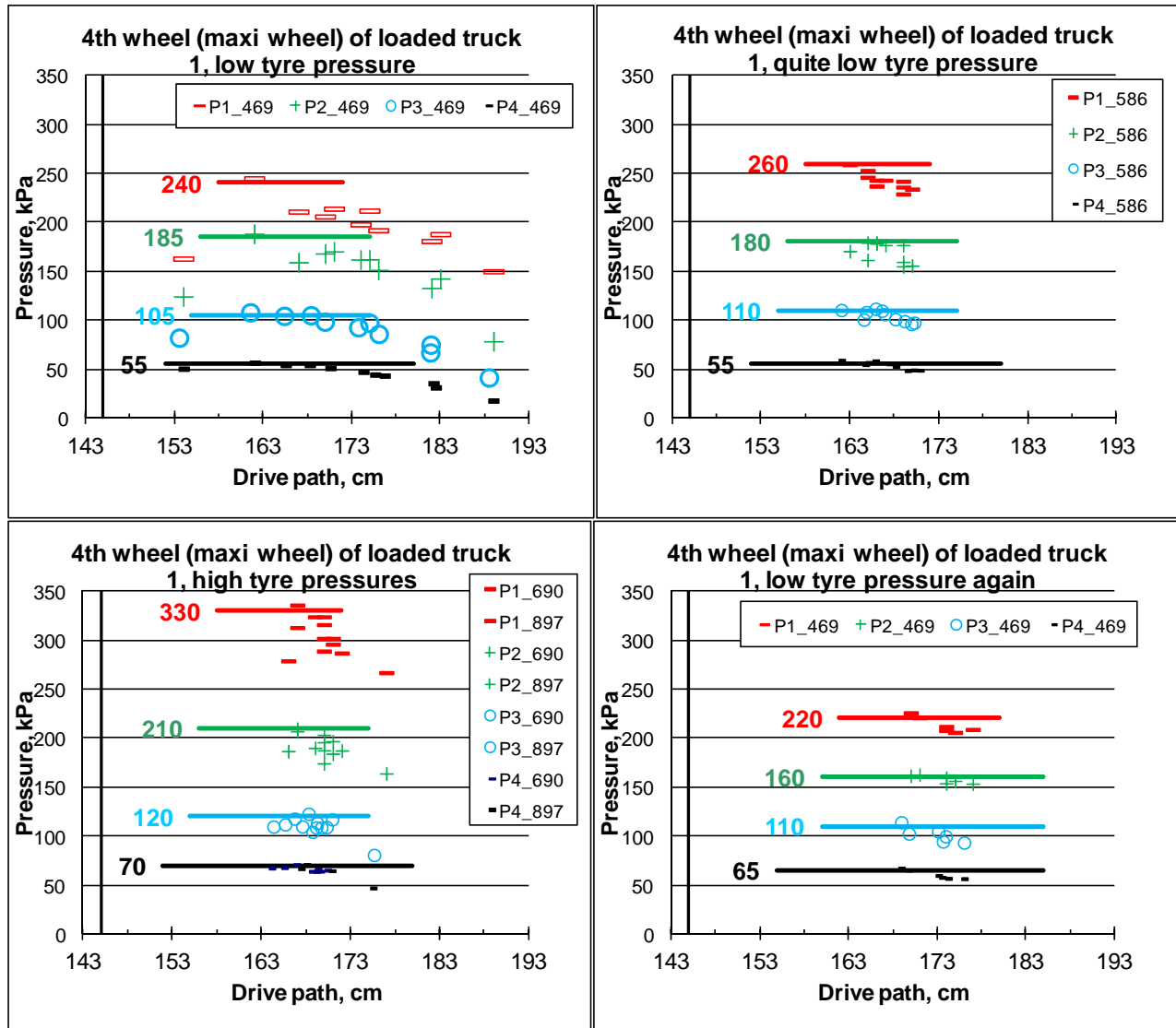


Figure 6.11 Earth pressures resulting from the maxi wheels of loaded Truck 1 at different depths. The four diagrams are in the same sequence as the truck passes. “Drive path” means the distance from the lasers.

6.1.2. Truck 2

6.1.2.1. Steering axle wheel

The wheel loads for the steering axle wheels of Truck 2 were approximately the same magnitude as those of empty Truck 1. The tyre pressure of the steering axle wheels in Truck 2 was however 690 kPa, i.e. less than the 814 kPa tyre pressure of Truck 1. Figure 6.12 shows that near to the

surface the highest measured earth pressure was about 310 kPa. This was lower than the measured earth pressure of 380 kPa from Truck 1, as a result of the wheel load being lower. The difference between the steering axle wheel of Truck 1 and that of Truck 2 was minimal at deeper earth pressures.

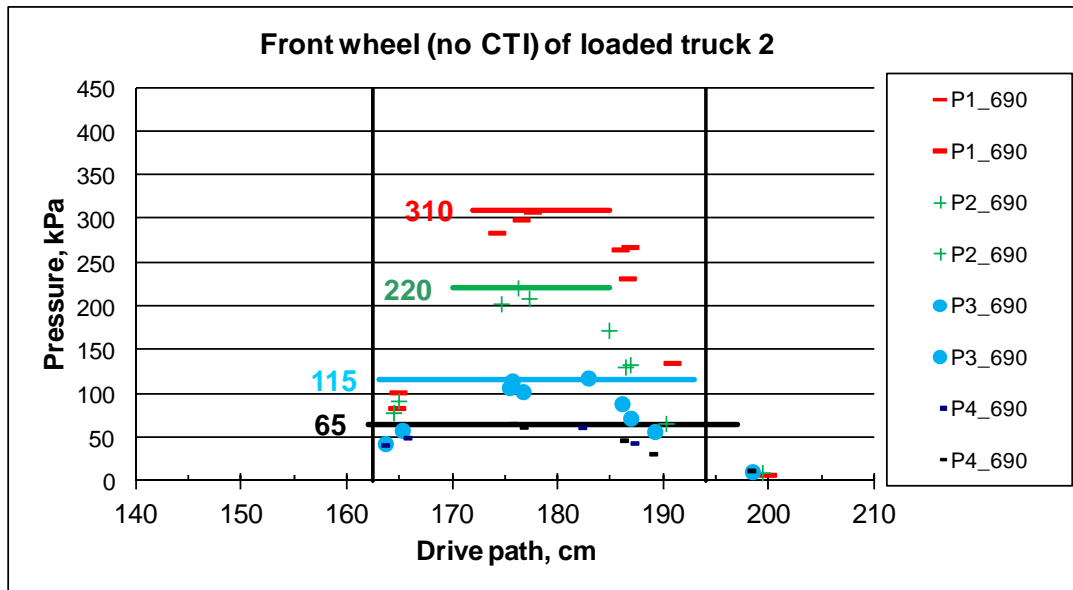


Figure 6.12 Earth pressures resulting from the steering axle wheel of loaded Truck 2 at different depths. “Drive path” means the distance from the lasers. The depths of the earth pressure cell were 67 (P1), 152 (P2), 248 (P3) and 389 mm (P4).

Truck 2 had two driving axles with twin wheels. Figure 6.13 shows the measured earth pressures at different depths due to the driving wheels of the loaded truck separately for low tyre pressure and quite high tyre pressure. The variation of the drive path was good for the low tyre pressure tests (on the left side of the figure), whereas on the right side (quite high tyre pressure) the wheels were effectively driving on only two paths as the road was rutting. Comparing the effect of different tyre pressures in the twin wheels was inconclusive as it was not possible to measure sufficient passes with high tyre pressure before the driving had to be stopped due to rutting and the effects of “crown driving” as illustrated earlier in Figure 6.6.

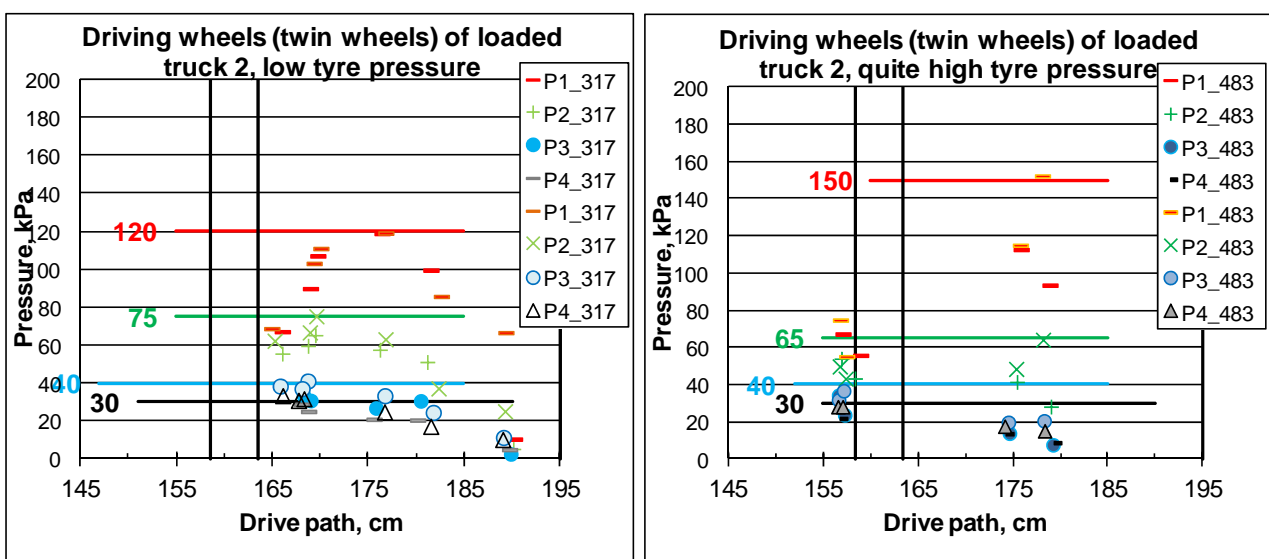


Figure 6.13 Earth pressures resulting from the twin wheels of loaded Truck 2 at different depths. The two diagrams are in the same sequence as the truck passes. “Drive path” means the distance from the lasers.

The trailer of Truck 2 had three axles with super single wheels. Figure 6.14 shows the measured earth pressures at different depths for these wheels separately for low and quite high tyre pressure. The variation of the drive path was generally good for the low tyre pressure tests (on the left side of the figure) whereas the quite high tyre pressure (on the right side of the figure) the wheels were driving effectively only two paths as the road was rutting such that only four passes were possible. The measured difference between the two tyre pressures was not remarkable. This might be due too few drive paths with high tyre pressures, or the accelerated rutting.

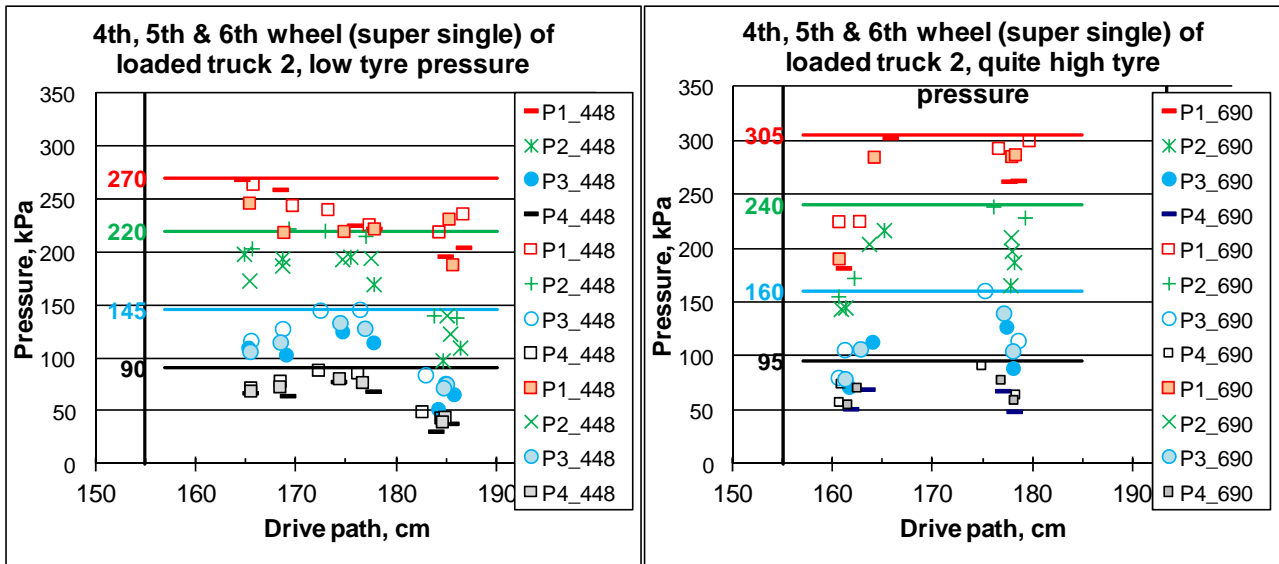


Figure 6.14 Earth pressures resulting from the super single wheels of loaded Truck 2 at different depths. The two diagrams are in the same sequence as the truck passes. “Drive path” means the distance from the lasers.

6.1.3. Difference between wheel types and the trucks

Figure 6.15 shows the highest measured earth pressures at different depths for a range of single wheels with wheel loads of 2300 kg to 3300 kg. The blue colour presents the measured values for the single wheel on the third axle of Truck 1 (2300 kg) with different tyre pressures. The green colour indicates the measured values on the single wheel of the first (steering) axle of Truck 2 (2800 kg) and the red colour shows the measured values on the single wheel of the first axle of unloaded Truck 1 (2700 kg). The difference between the green and red values is quite clear near the surface as the tyre pressure of steering axle wheel was about 120 kPa lower. This difference however begins to vanish at 150 mm depth.

Figure 6.16 shows the highest measured earth pressures at different depths for a range of maxi and super single wheels with wheel loads of approximately 4200 kg. The blue colour presents the measured values for the maxi wheels of Truck 1 with different tyre pressures. The brown colour shows the super single wheels of Truck 2. It can be seen from the figure that the measured earth pressures were significantly higher under the super single wheels than under the maxi wheels when low tyre pressures were used. The difference ranged from 25 kPa to almost 50 kPa.

When comparing the measured earth pressures between “high” or “quite high” tyre pressures of maxi wheels and super single wheels it has to be borne in mind that the values for the super single wheels were obtained from four passes on two driving paths. Even then, it seems that the measured earth pressures under the super single wheels were higher than under the maxi wheels.

One uncertainty in the comparison arises from the width of the maxi wheel and particularly if the edges of the maxi wheels were spreading more stresses into soil around the developing rut than the thinner super single wheels. Irrespective of this doubt, it seems that maxi wheels are more road friendly than super single wheels if the rutting is developing under the base course.

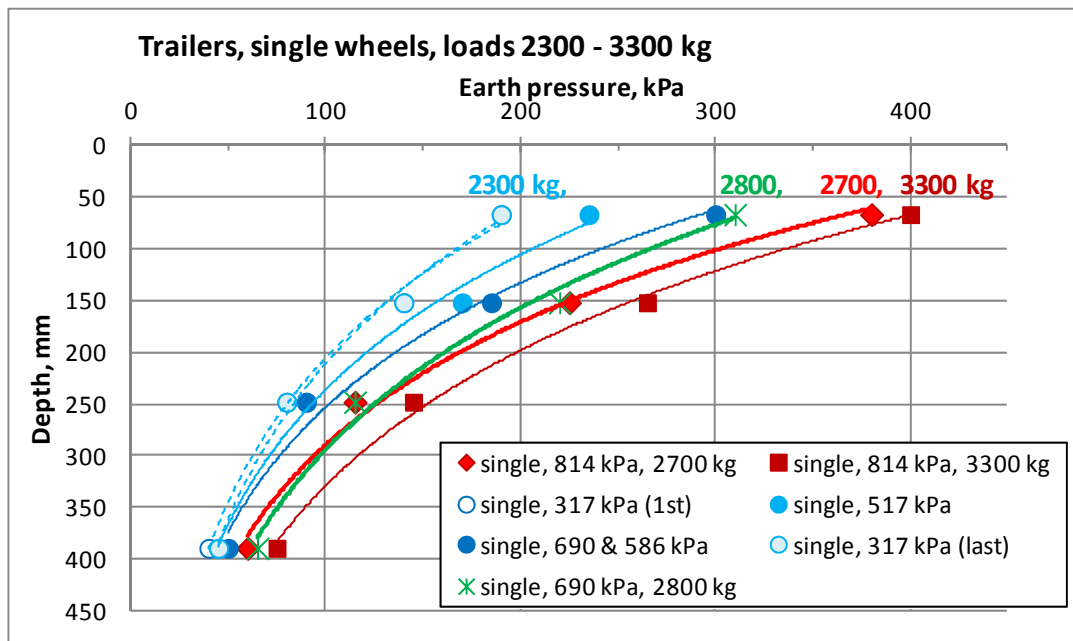


Figure 6.15 Highest earth pressures resulting from single wheels at different depths. Blue represents the single wheel on the 3rd axle of Truck 1, green represents the steering axle wheel of Truck 2, and red and brown are steering axle wheels of Truck 1.

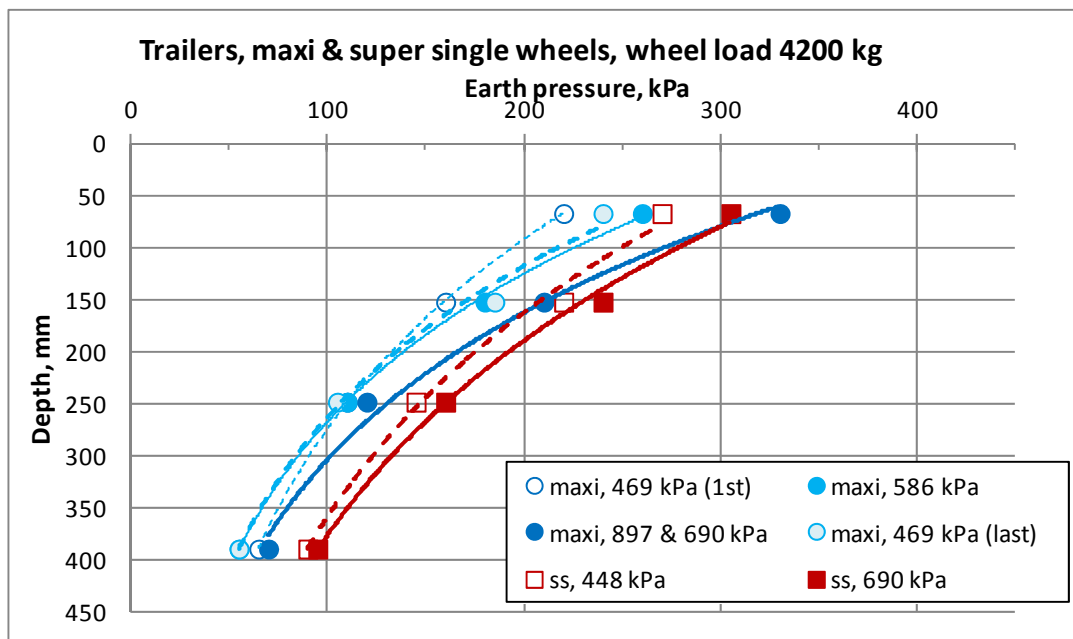


Figure 6.16 Highest earth pressures resulting from the maxi and super single wheels of the trailers at different depths. Blue is Truck 1, and brown is Truck 2.

Figure 6.17 shows the highest measured earth pressures at different depths for a range of single and super single wheels. The blue colour presents the measured values for the super single wheels of the trailer of Truck 2 with wheel loads of approximately 4200 kg. The red colours are the steering axle wheels (single) of Trucks 1 and 2 with wheel loads of 2700 kg and 3300 kg. It can be seen that the measured earth pressures of the super single wheel and single wheel with the same tyre pressure were about the same near the road surface even though wheel load of the super single wheel was 50 % higher. When the tyre pressure of the single wheel increased the earth pressure was greater for a single wheel than for a super single wheel near the road surface. The measured earth pressure of super single wheels was higher at deeper layers (at 390 mm).

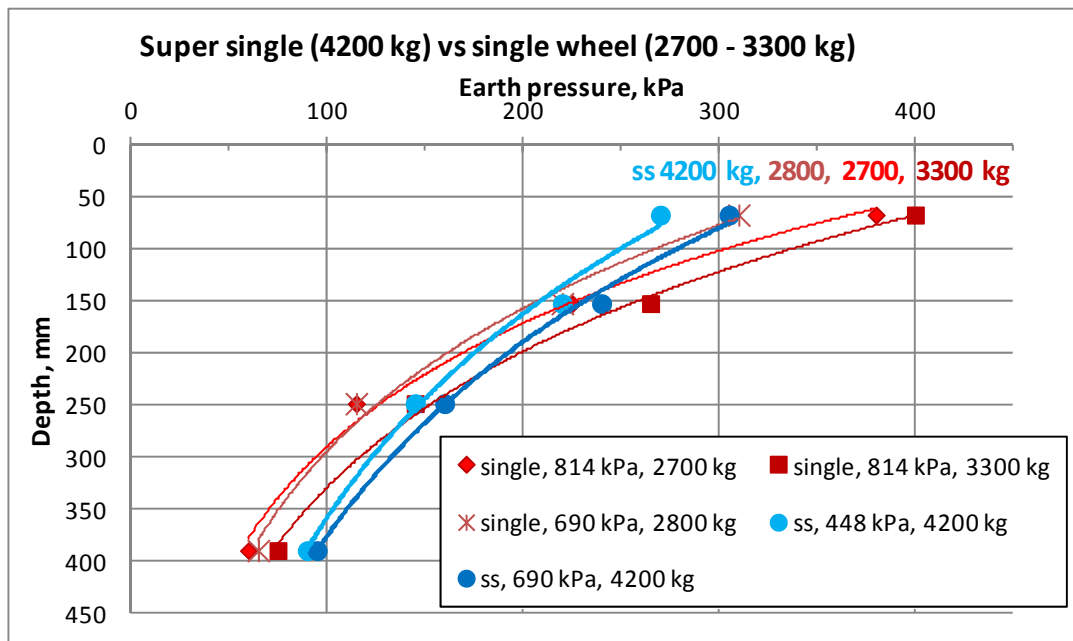


Figure 6.17 Highest earth pressures resulting from single and super single (ss) wheels at different depths. Blue represents the super single wheels of Truck 2. The red lines are single wheels of Trucks 1 and 2.

Figure 6.18 shows the highest measured earth pressures at different depths for single and maxi wheels. The blue colour presents the measured values for the maxi wheels of Truck 1 with a wheel load of approximately 4200 kg. The red colours represent the steering axle wheels (single) of Trucks 1 and 2 with wheel loads from 2700 kg to 3300 kg. It can be seen that the measured earth pressures of the maxi wheels were lower, or about the same, than the measured pressures for single wheels with same tyre pressure even though the wheel load of the maxi wheel was 50 % higher. When the tyre pressure of the single wheel was increased the earth pressure was greater for a single wheel than for a maxi wheel near the road surface. The measured earth pressure of maxi and single wheels was about the same at deeper layers (at 390 mm).

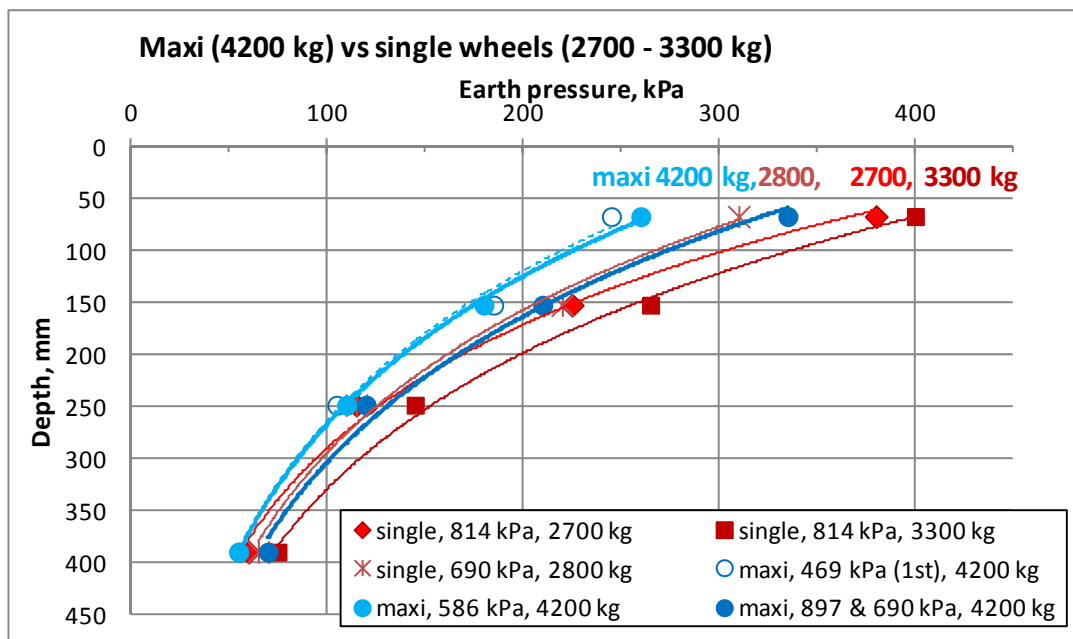


Figure 6.18 Highest earth pressures resulting from single and maxi wheels at different depths. Blue is maxi wheels of Truck 1, reds are steering axle wheels (single) of Trucks 1 and 2.

6.2. STRAIN GAUGE MEASUREMENTS

The distance between the strain gauge plates before the test was approximately 120 mm. Figure 6.19 shows the deformation between the plates after each passage of the trucks. After the test the permanent deformation near the road surface was almost 10 %.

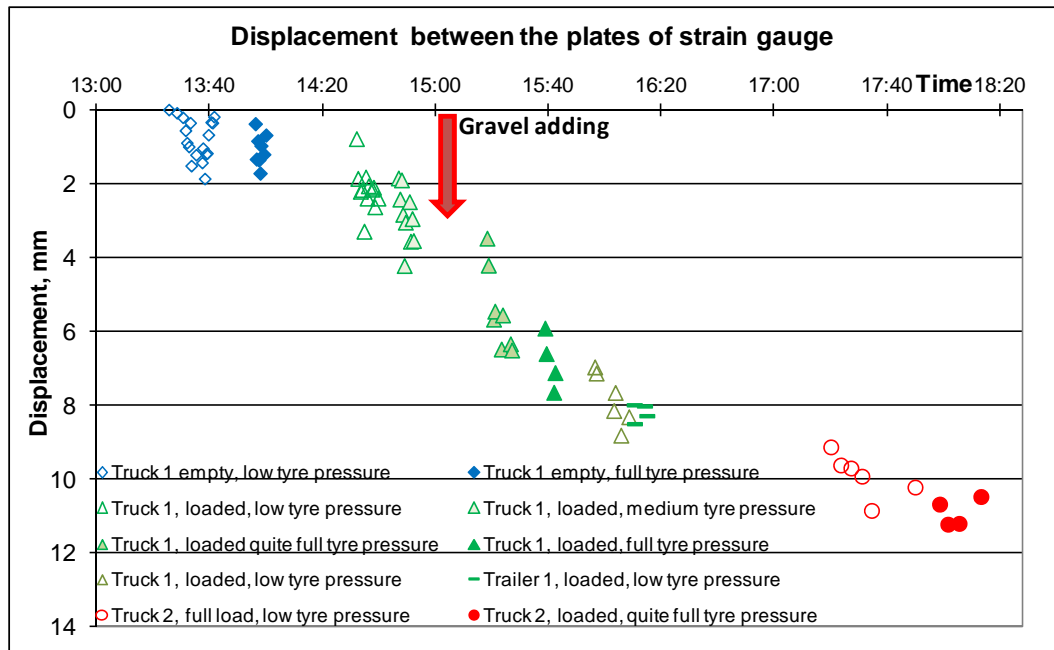


Figure 6.19 Deformation between strain gauge plates after each pass of the trucks.

Figure 6.20 illustrates how the strains were calculated for each wheel pass from the measured data from the strain gauge by determining the highest and lowest value for each wheel pass. This method gives some inaccuracies in the calculated values but presents all passes alike. The driving direction, forward or reverse, produced some variation in the measured data. Also the increasing densification of the layers over the course of the tests had an influence on the measured values, which complicated the comparison between the different tyre pressures. The reversing manoeuvres were taken into account in the calculations for Truck 1. Some scattering remained in the data due to the waiting time between the truck passes. The permanent deformation of the layer can be seen in the presented figures. The strain was taken to be the amplitude of each wheel. The resilient strain was calculated by subtracting the permanent strain from the overall strain. It has also to be remembered that the driving speed was quite slow.

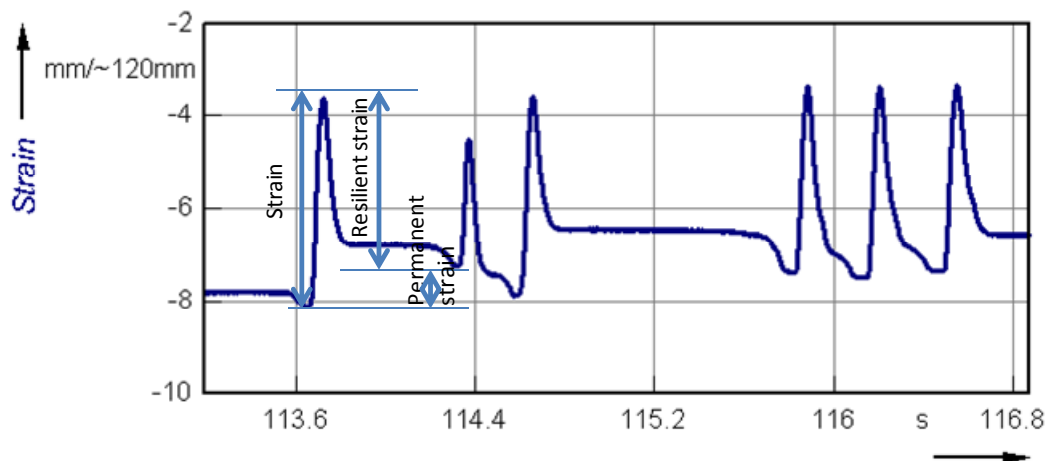


Figure 6.20 Diagram showing the calculated strains for the wheels from the measured data.

Figure 6.21 shows that the measured strains under the steering axle wheels increased from 0.026 to 0.042 as the wheel load increased from 2700 kg to 3300 kg (The tyre pressure of the steering axle wheels did not change during test). Some of the difference seen might be due to the more uneven road as the test progressed. It was not possible to draw a clear trend between tyre pressures and wheel loads for the twin wheels from the measured data. The highest strains of the twin wheels were between 0.025 and 0.029 as can be seen from Figure 6.22. Figure 6.23 shows the measured strains under the single wheels of the third axle of Truck 1. This Figure shows that the strain increased by about 50 % as the tyre pressure was increased from 317 kPa up to 690 kPa. When the tyre pressure was decreased down to low, the measured strains decreased but remained about 25 % higher than the earlier measured level with low tyre pressure.

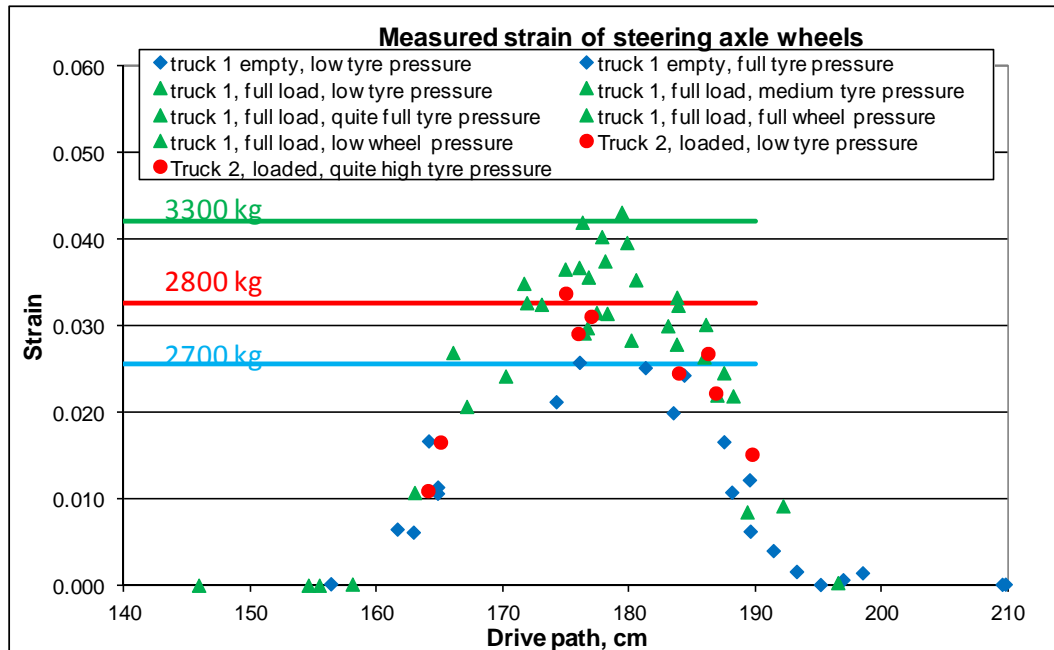


Figure 6.21 Strains from the passes of steering axle wheels. Steering axle wheels did not have CTI. Wheel loads were approximately 3300, 2800 and 2700 kg.

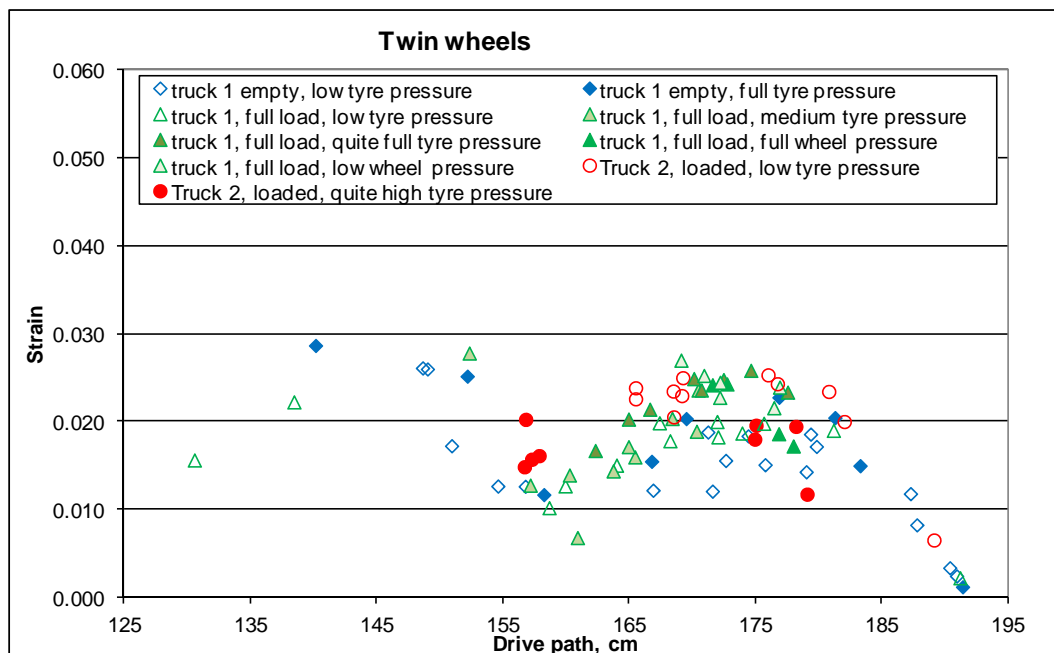


Figure 6.22 Strains from the passes of the Trucks 1 twin wheels.

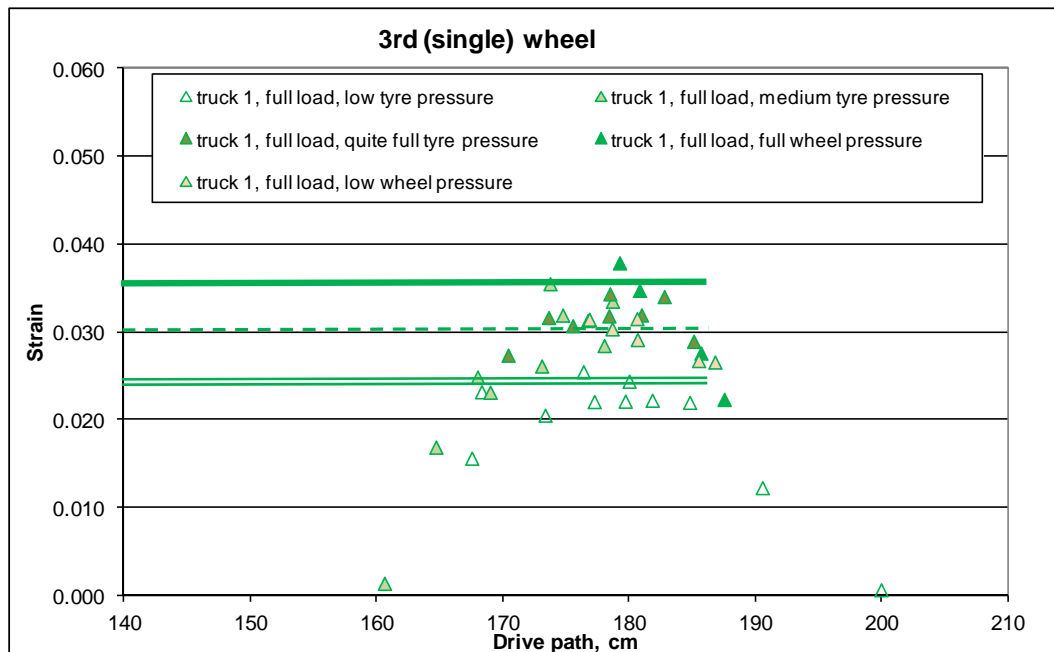


Figure 6.23 Strains from the passes of Truck 1 third wheels (single).

Figure 6.24 shows that the measured strains of the maxi wheels increased as the wheel load increased, or the tyre pressure of the full load truck increased. There were no significant differences between low or full tyre pressure for empty Truck 1 as the wheel load was low. The strain levels of the maxi wheels were lower than the strain levels of the steering axle wheels. Figure 6.25 shows the measured strains of the super single wheels. No remarkable difference was measured between low and full tyre pressure. The strain level was about the same as with maxi wheels.

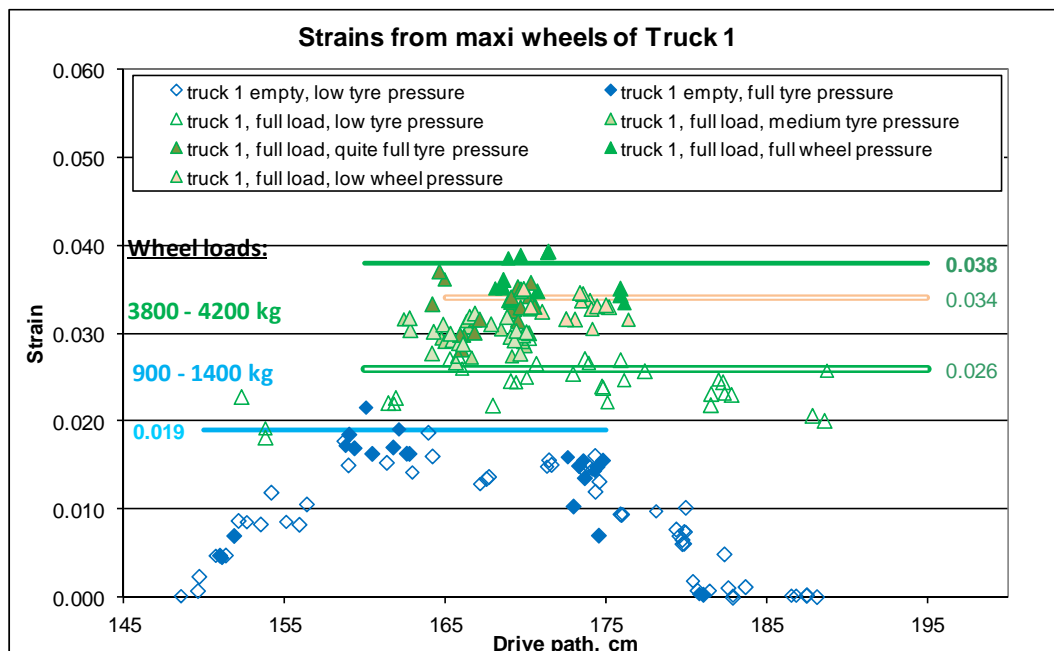


Figure 6.24 Strains from the passes of Truck 1 maxi wheels (trailer). Wheel loads of the full trailer were 3800 - 4200 kg and empty trailer 900 - 1400 kg.

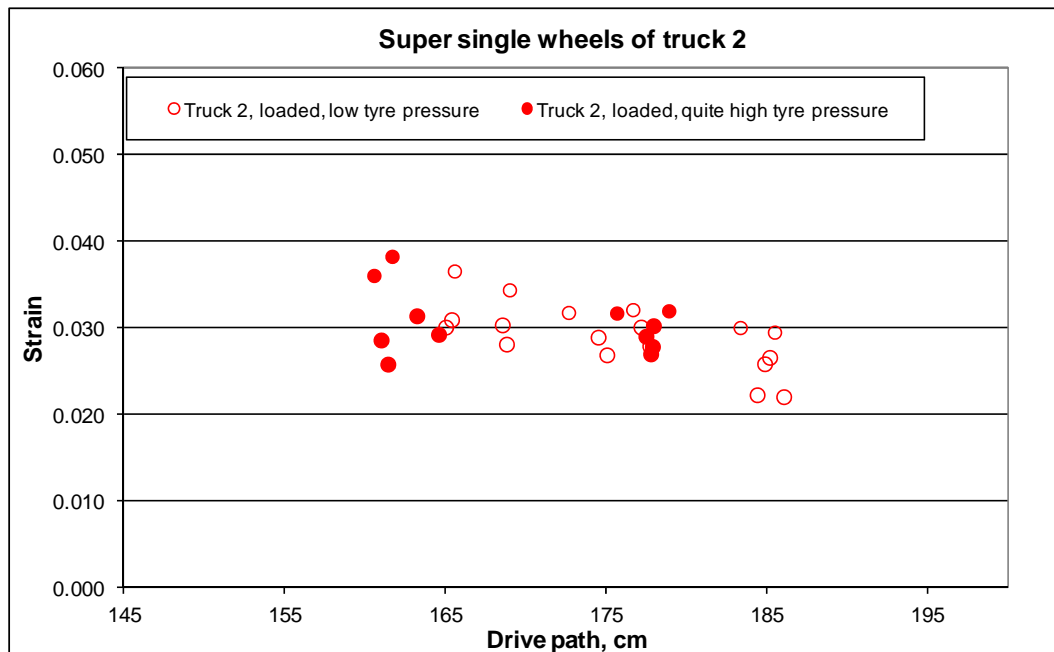


Figure 6.25 Strains from the passes of Truck 2 super single wheels (trailer). Wheel loads were 3700 – 4200 kg.

Figure 6.26 shows that the measured highest resilient strains of the steering axle wheels increased as wheel load increased from 2700 kg to 3300 kg. (The tyre pressure of the steering axle wheels was not changed.) The scatter of resilient strains increased as the test progressed. The blue dots (empty Truck 1) are evenly spread across the drive path and the green dots (full Truck 1) are mainly between 2.0 and 3.2 %. The red dots of empty Truck 2 are nearer the green dots of full Truck 1 than the blue full Truck 2 despite the wheel loads of the empty trucks being fairly similar. It seems that unevenness of the road surface has had an influence on the measured resilient strains. It was not possible to draw a clear trend between tyre pressures and wheel loads from the measured data of twin wheels as Figure 6.27 shows. The highest resilient strains for twin wheels were about 3 % for the loaded trucks, and less than 2.5 % for the empty Truck 1.

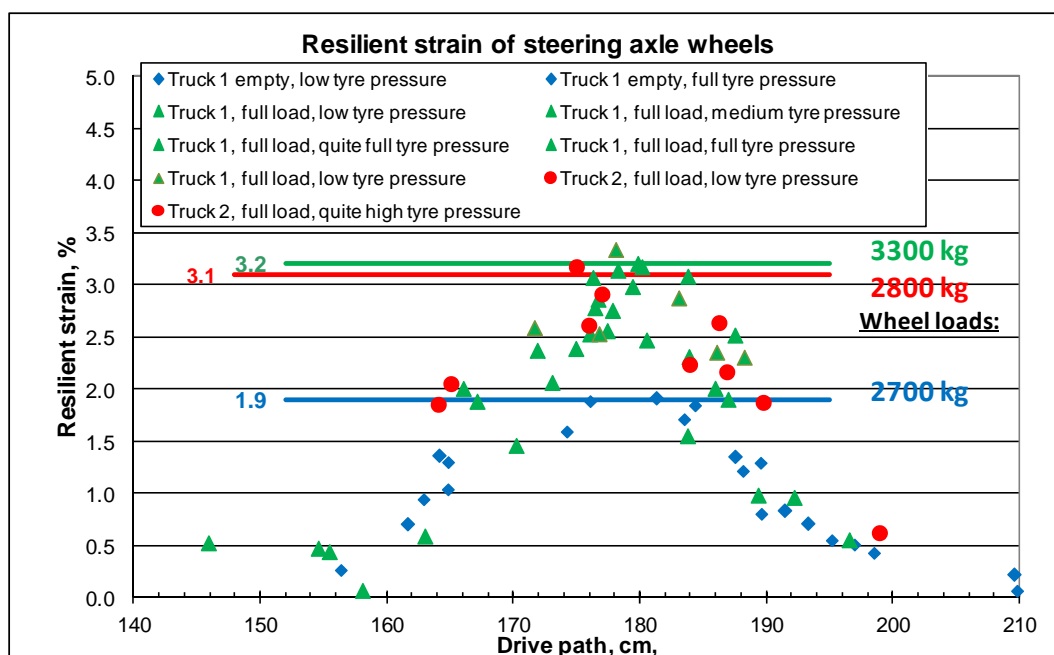


Figure 6.26 Resilient strains from the passes of steering axle wheels. Steering axle wheels did not have CTI. Wheel load were about 3300 (green), 2800 (red) and 2700 (blue) kg.

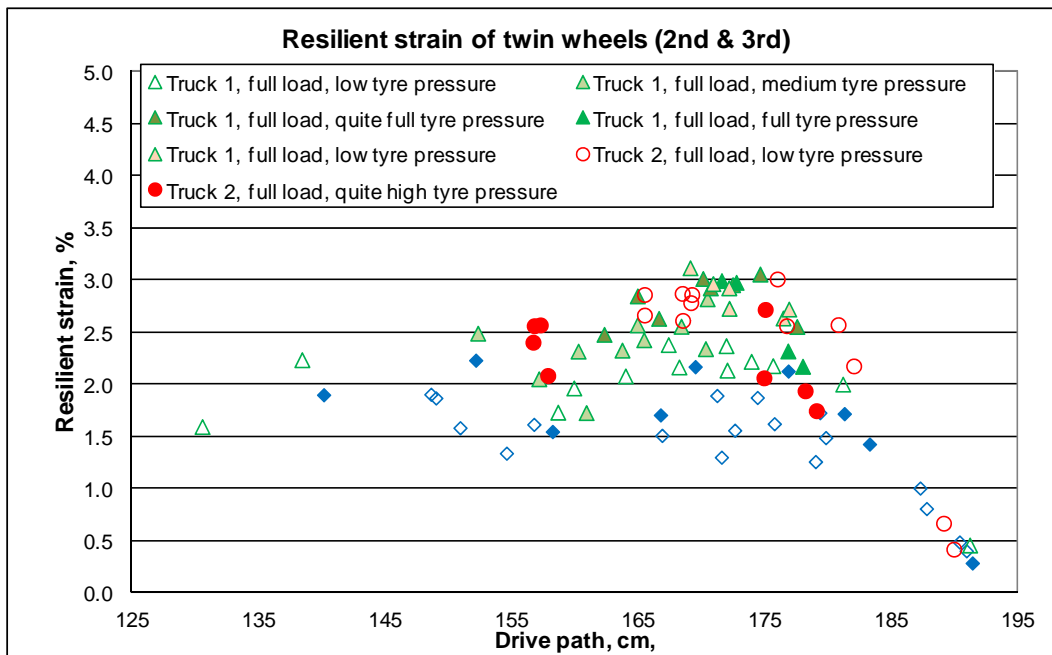


Figure 6.27 Resilient strains from the passes of twin wheels.

Figure 6.28 shows the measured resilient strains for the single wheels of the third axle of Truck 1. The figure shows that the resilient strain increased about 40-50 % as the tyre pressure was increased from 317 kPa up to 690 kPa. When the tyre pressure was reduced to low, the measured resilient strains decreased a little but remained much higher than the earlier measured level with low tyre pressure

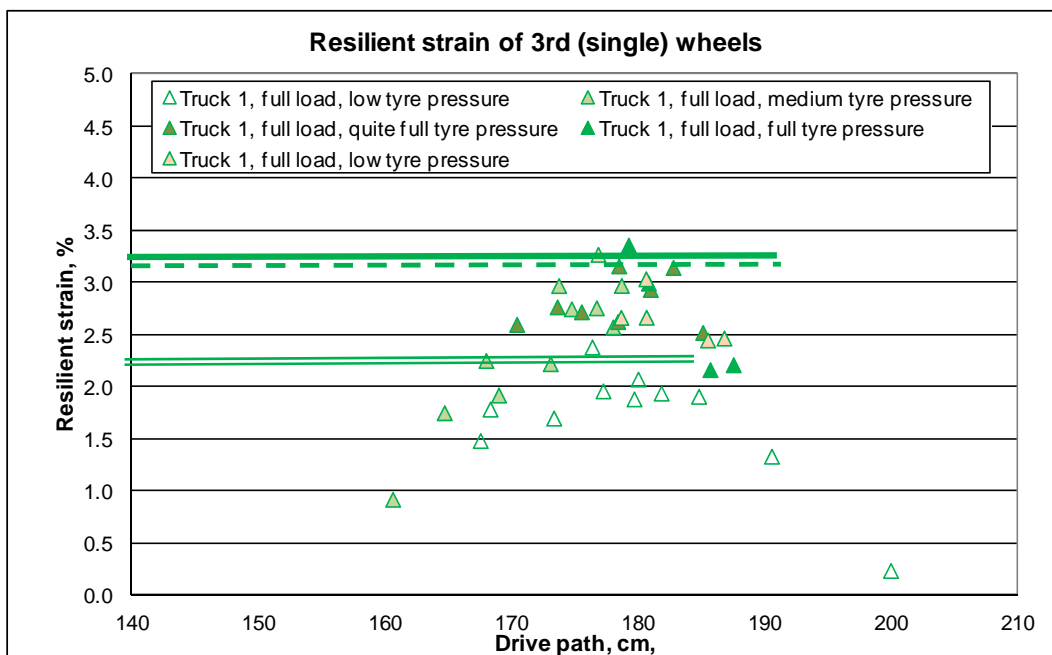


Figure 6.28 Resilient strains from the passes of truck 1 third wheels (single).

Figure 6.29 shows that the measured resilient strains of the maxi wheels increased as the wheel load increased, or the tyre pressure of the full load truck increased. There were no differences between low or full tyre pressures for empty Truck 1 when the wheel load was low. The resilient strain levels for maxi wheels with medium or high tyre pressure were higher than the resilient strain level for steering axle wheels. Figure 6.30 shows that the measured strains and the resilient strains for super single wheels were slightly lower with low tyre pressure, but no remarkable difference was measured. The resilient strain level (2.9 %) was lower than with maxi wheels (3.5 – 3.9 %).

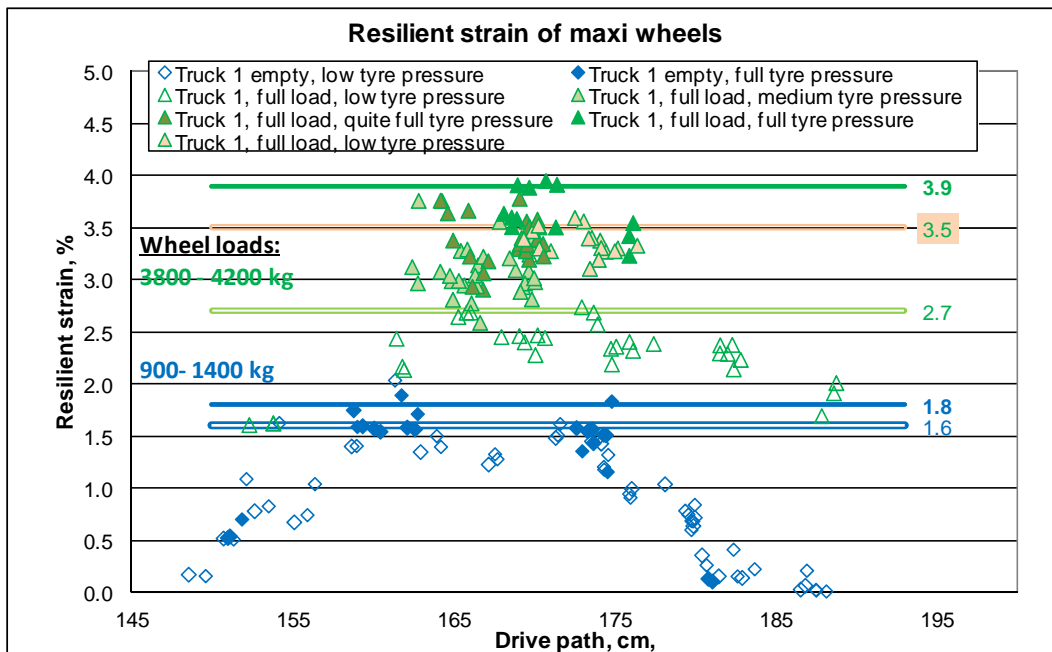


Figure 6.29 Resilient strains from the passes of Truck 1 maxi wheels (trailer). Wheel loads of full trailer were 3800 - 4200 kg and empty trailer 900 - 1400 kg.

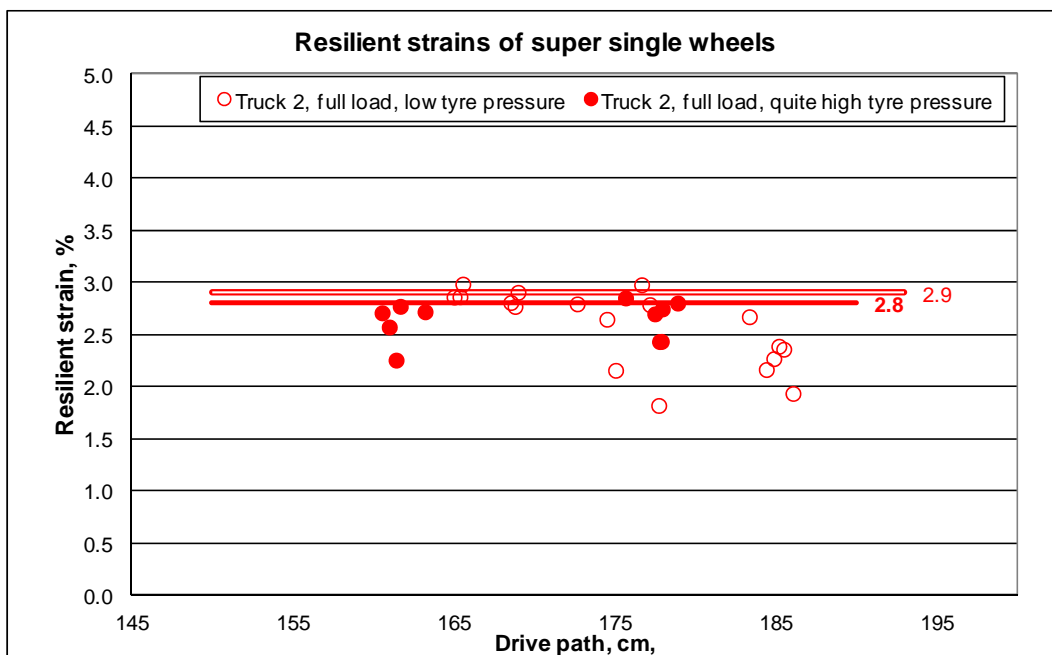


Figure 6.30 Resilient strains from the passes of Truck 2 super single wheels (trailer). Wheel loads were 3700 - 4200 kg.

Figure 6.31 shows that the measured highest permanent strains for steering axle wheels were about 1.3 %. (The tyre pressure of steering axle wheels was not changed during the test.) The scatter of permanent strains was quite high. It seems that the highest permanent strains were achieved when the drive path was about 180 cm, and it can be assumed that the tyre is above the strain gauge at this point. Where the measured drive path was less than 165 cm or greater than 190 cm the permanent strain could be below zero, resulting from wheel load pushing material between the strain gauge plates causing the measured permanent strain to be negative.

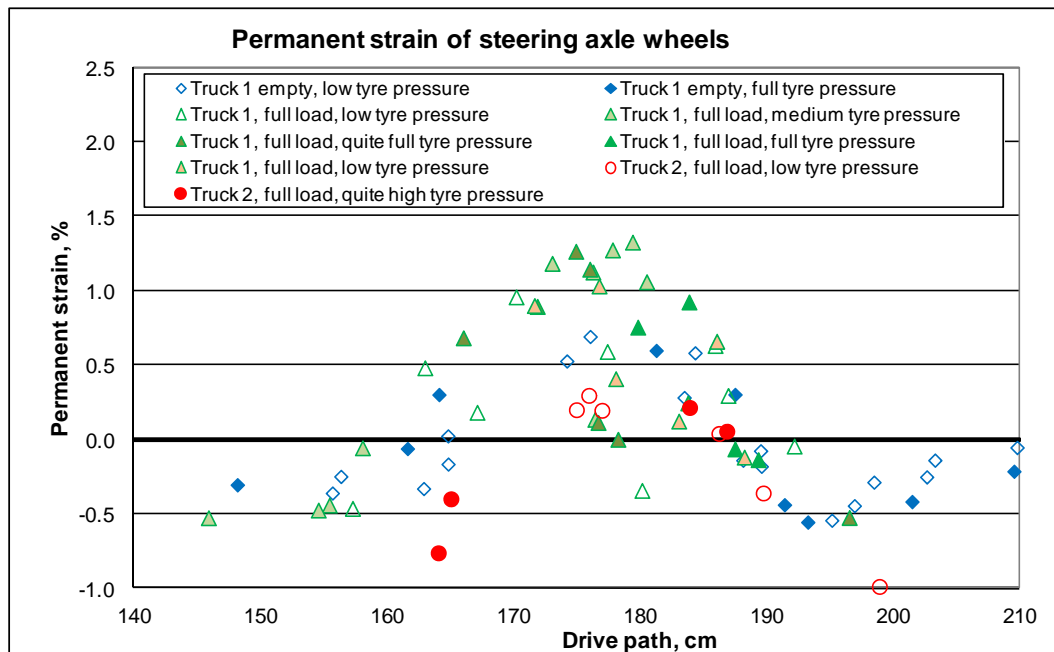


Figure 6.31 Permanent strains from the passes of steering axle wheels. Steering axle wheels did not have CTI. Wheel load were about 2700 kg (blue), 3300 kg (green) and 2800 kg (red).

Figure 6.32 shows that the measured highest permanent strains of the driving (twin) wheels were less than 1 %. The tyre pressure did not seem to have an effect on the permanent strain. Mostly the permanent strain was negative. This might originate from the position of the twin wheel on the crown of the road. The third axle of the Truck 1 had a single wheel and the measured permanent strain is shown in Figure 6.33. The permanent strains were mainly 0 – 0.5 %. Tyre pressure might have had a small effect on the permanent strain as the highest strains of about 0.55 % were from the passes of medium to full tyre pressure, and the highest permanent strains from passes with low tyre pressure were about 0.4 %.

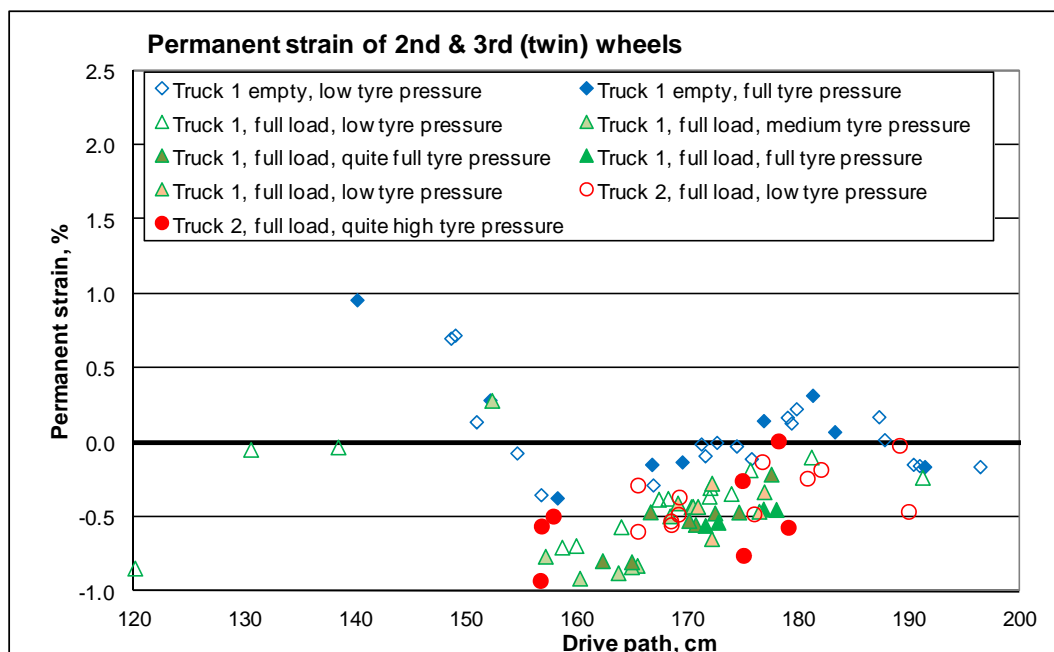


Figure 6.32 Permanent strains from the passes of driving (twin) wheels. Wheel load were about 4300-4800 kg (blue), 4000 kg (green) and 3600-4300 kg (red).

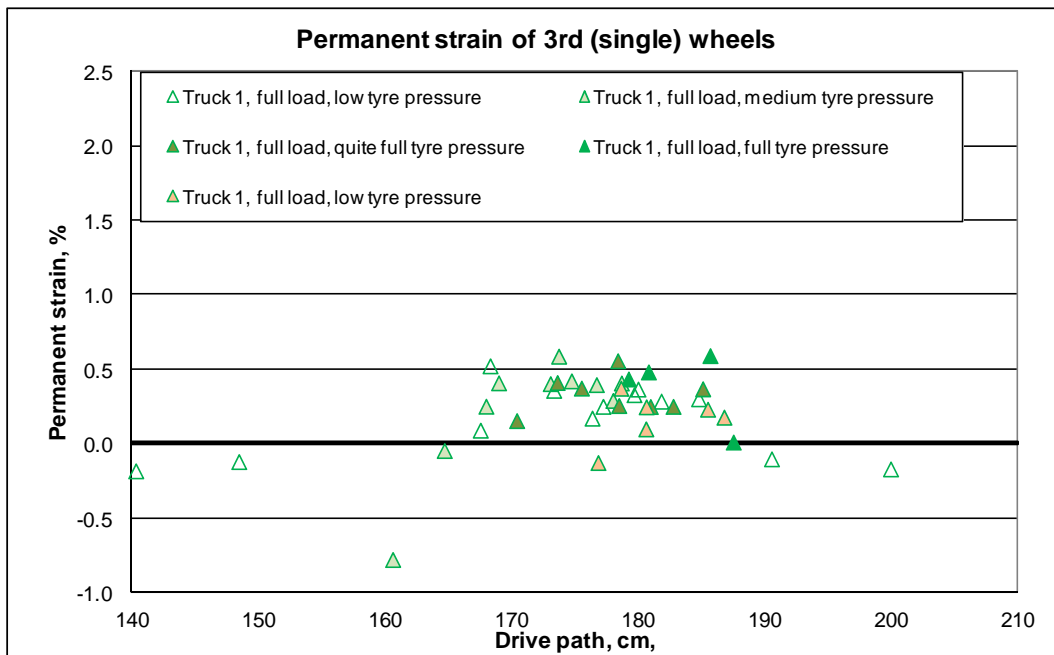


Figure 6.33 Permanent strains from the passes of the third (single) wheels of the loaded Truck 1. Wheel loads were about 2500 kg.

Figures 6.34 - 6.36 show the permanent strains from the passes of the trailers with maxi or super single wheels. The permanent strains of empty trailer 1 with maxi wheels varied from -0.5 % to +0.5 %, with an average of near zero (Figure 6.34). The permanent strains of the loaded trailer 1 with maxi wheels varied from -0.7 % to +0.5 %, with the average below zero (Figure 6.35). The permanent strains of the loaded trailer 2 with super single wheels varied from 0.0 % to +10 %, with the average about +0.4 % (Figure 6.36). It seems that the super single wheels caused more permanent deformation than the maxi wheels on the test site. According to Figures 6.34 - 6.36 the tyre pressure did not have an effect on the measured permanent strain on the test site.

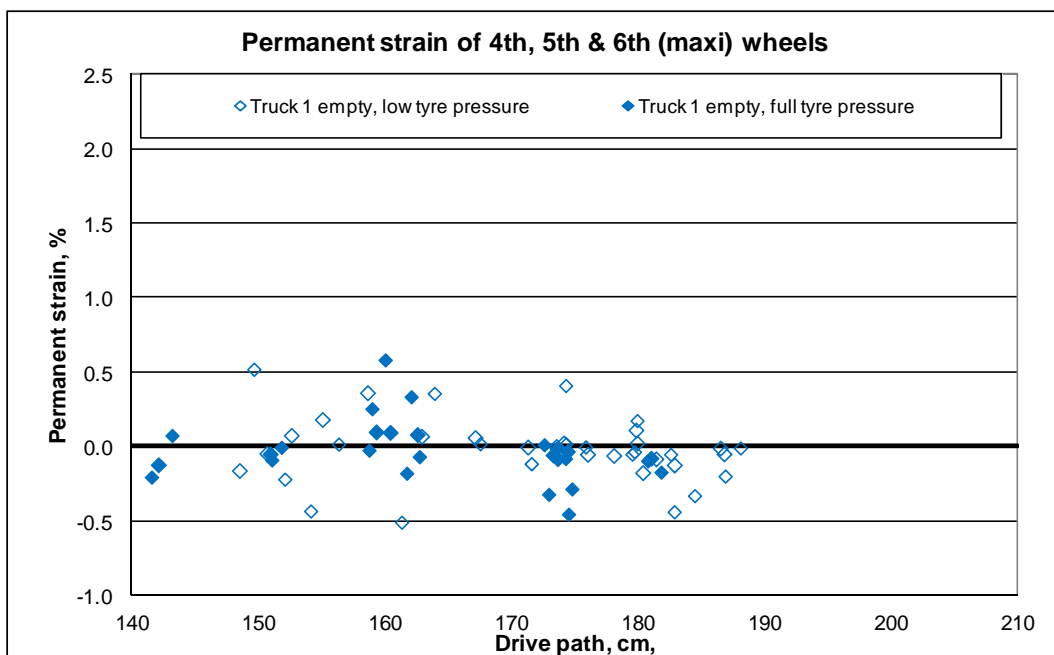


Figure 6.34 Permanent strains from the passes of the maxi wheels of the empty Truck 1. Wheel load were 850-1400 kg.

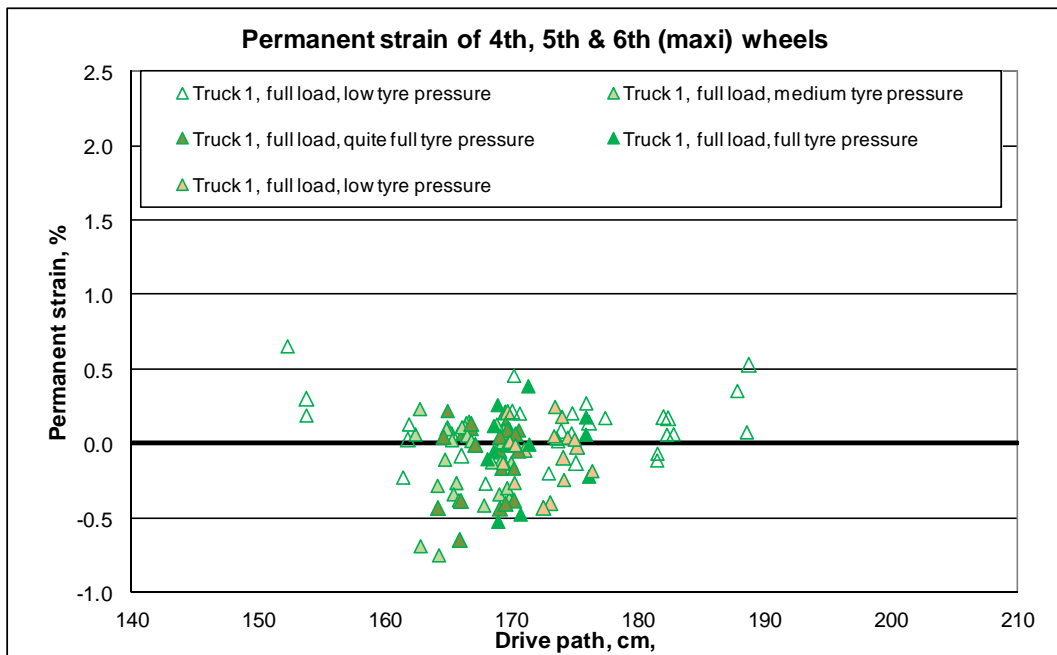


Figure 6.35 Permanent strains from the passes of the maxi wheels of the loaded Truck 1. Wheel load were 3800-4200 kg.

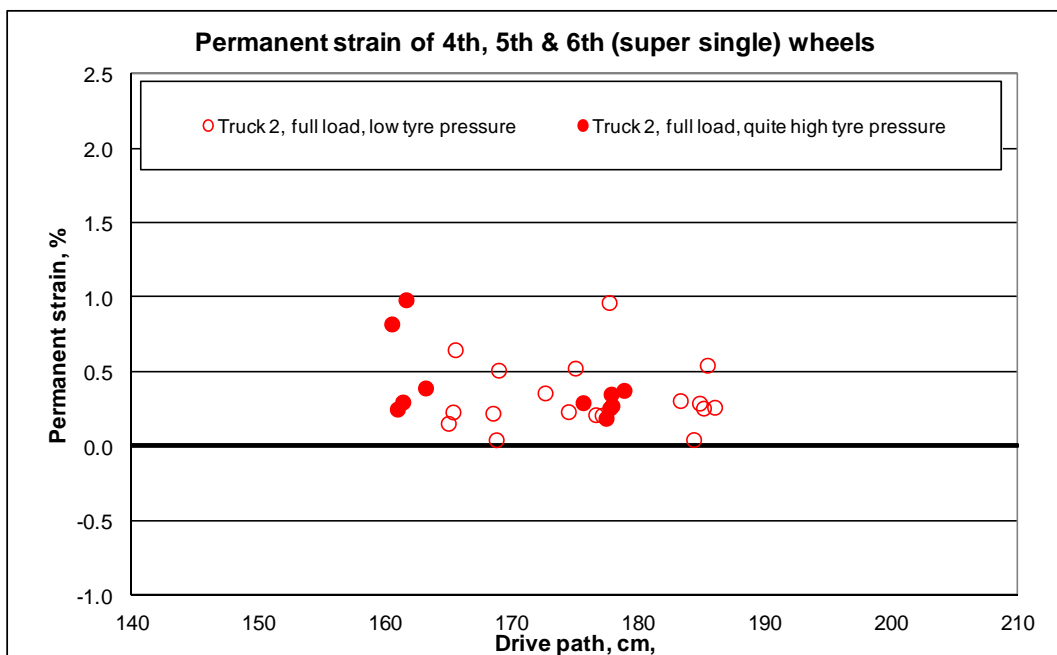


Figure 6.36 Permanent strains from the passes of the super single wheels of the loaded Truck 2. Wheel load were 3700-4200 kg.

Figures 6.37 - 6.39 show the permanent strains from the passes of the trailers axle by axle. The permanent strains of the 4th axles varied from -0.3 % to +1.0 %, and the highest permanent strains were caused by super single wheels (Figure 6.37). The permanent strains of the 5th axles were mainly between -0.1 and +0.3 %, and the highest permanent strains were again from the super single wheels (Figure 6.38). The permanent strains of the 6th axles varied from -0.7 % to +1.0 %, and the highest permanent strains were not clearly from the super single wheels (Figure 6.39). The variation of the permanent strains was highest on the 6th axle, which might partly be due to the recovery time before the next wheel was measured.

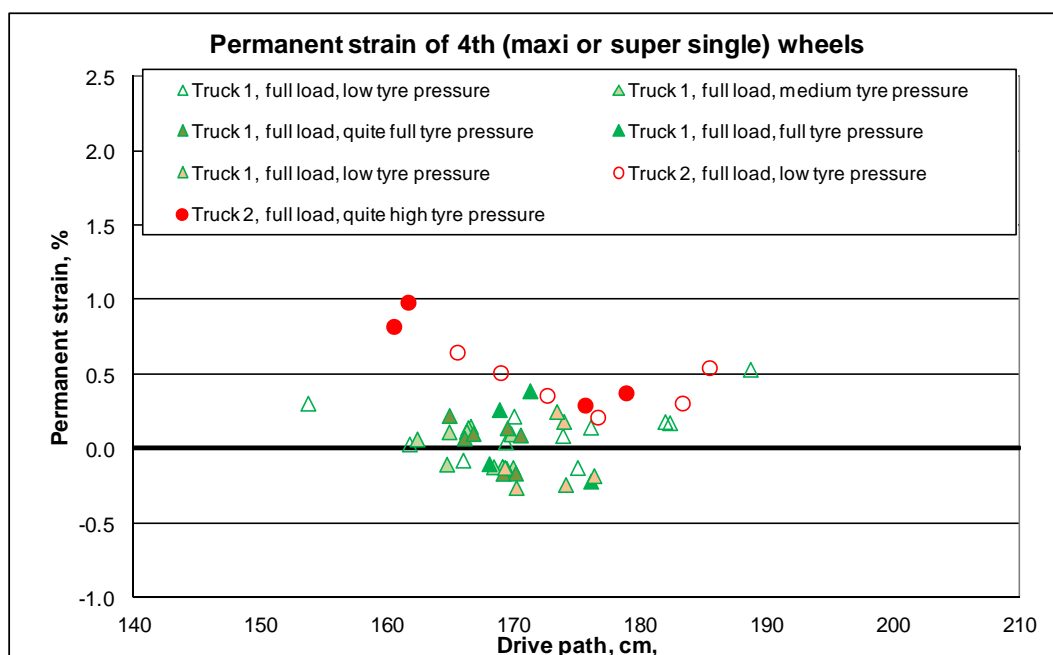


Figure 6.37 Permanent strains from the passes of the 4th axle. Truck 2 (red dots) had super single wheels.

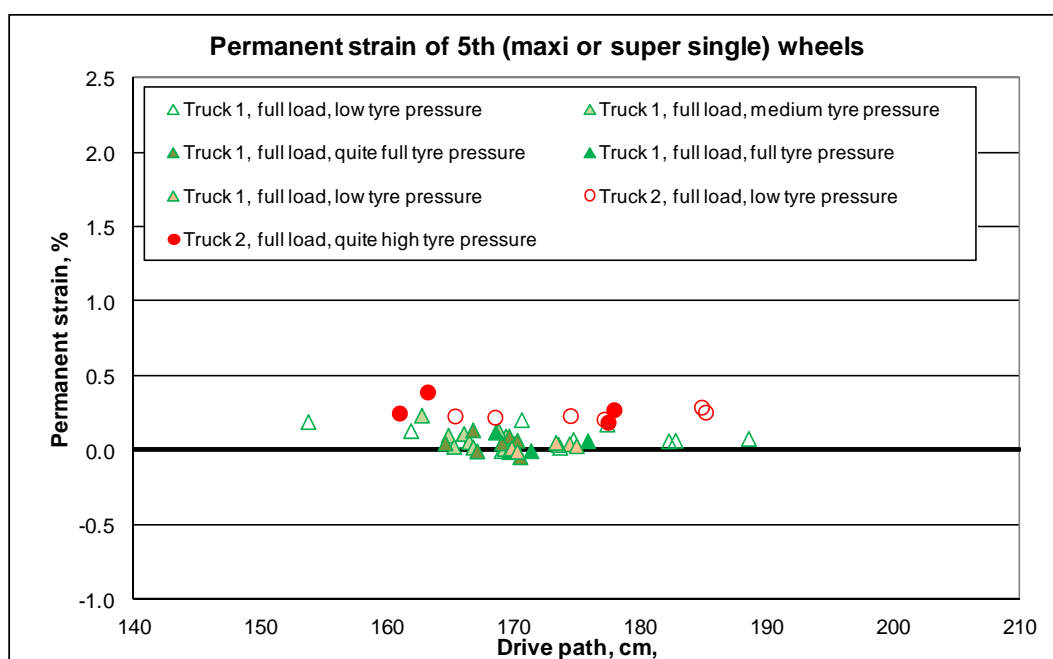


Figure 6.38 Permanent strains from the passes of the 5th axle. Truck 2 (red dots) had super single wheels.

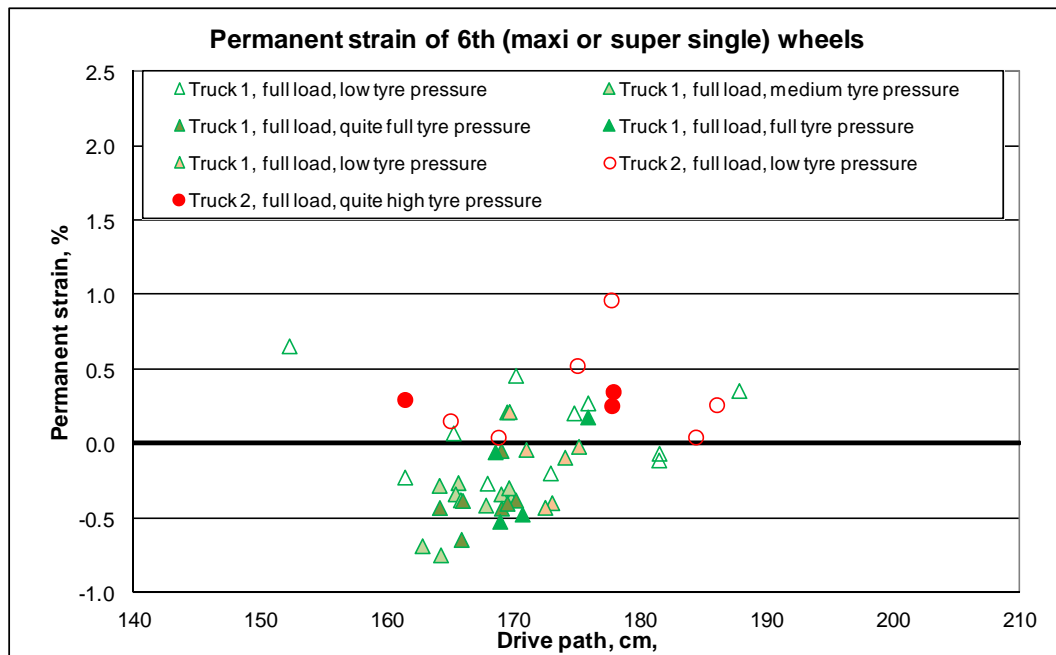


Figure 6.39 Permanent strains from the passes of the 6th axle. Truck 2 (red dots) had super single wheels.

6.3. RUTTING AND DEFORMATIONS ON THE ROAD SURFACE

The elevation of the road surface was measured using an engineer's level. The reference points were on fixed hard points on both sides of the road about 10 metres off the road. Figure 6.38 shows the changing elevation by position after the loadings. When the gravel regulating material is taken away from the road level it can be seen that the driving path had settled by 10 mm to 35 mm over the course of the test. It is possible that the act of adding gravel to the road to infill the ruts may have caused the road surface to be a little bumpier.

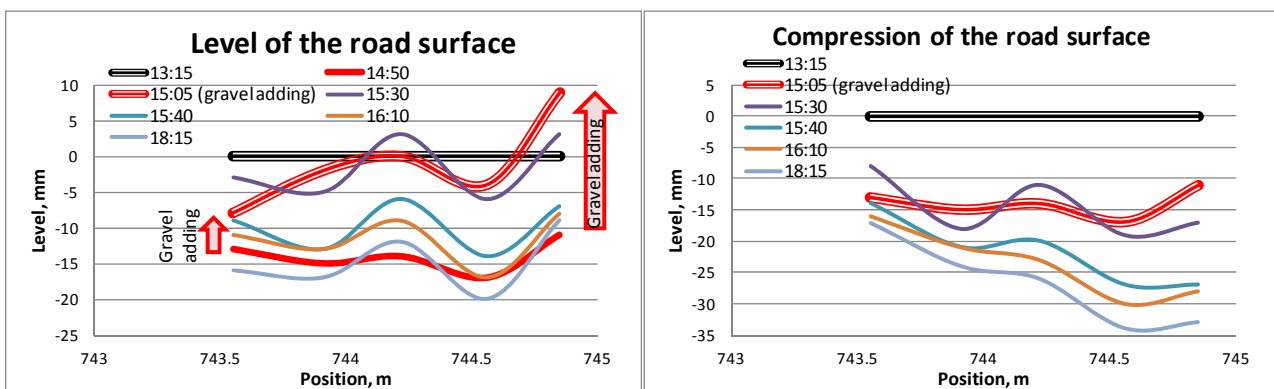


Figure 6.40 Level of the road surface on the test site. The diagram on the left hand side shows the measured level and the diagram on the right hand side with the gravel regulating deducted.

7. ANALYSIS OF THE MEASUREMENTS

7.1. MODULUS

The measured data allowed a modulus to be calculated for the road. Earth pressure cell P1 (depth 67 mm) was at the level of the strain gauge (34-158 mm) and it was decided that it was the most appropriate cell to represent the average loading for the strain gauge layer. Cell P1 was however located 0.7 m from the strain gauge and in view of this it was decided to limit the range of drive paths considered. If the drive path across cell P1 differed by more than 10cm from the drive path across the strain gauge the values would be removed from the data.

Figure 7.1 shows the calculated resilient modulus from the measured data of steering axle wheels in relation to the drive path. For the drive path 165 – 190 cm the resilient modulus was mainly 10 – 20 MPa.

Figure 7.2 shows the same resilient modulus in relation to the measured earth pressure. (The steering axle wheels did not have CTI). The loading order for the wheel loads were 2700 kg (blue), 3300 kg (green) and 2800 kg (red). It can be seen that at the beginning of the loading the resilient modulus was higher. The probable reason for this was that the layer near the surface became more plastic with the number of truck passes, and the increasing loads, with the result that the resilient modulus decreased. The difference in resilient modulus between the passages of full trucks became insignificant.

Figure 7.3 shows the calculated resilient modulus from the measured data of twin wheels in relation to the drive path. The resilient modulus was below 15 MPa in all cases, and the highest values were achieved when the wheel was nearest the roadside, i.e. the wheel was not on the crown. Figures 7.4 and 7.5 present the same resilient modulus calculated for maxi and super single wheels and show the resilient modulus to be about 10 MPa.

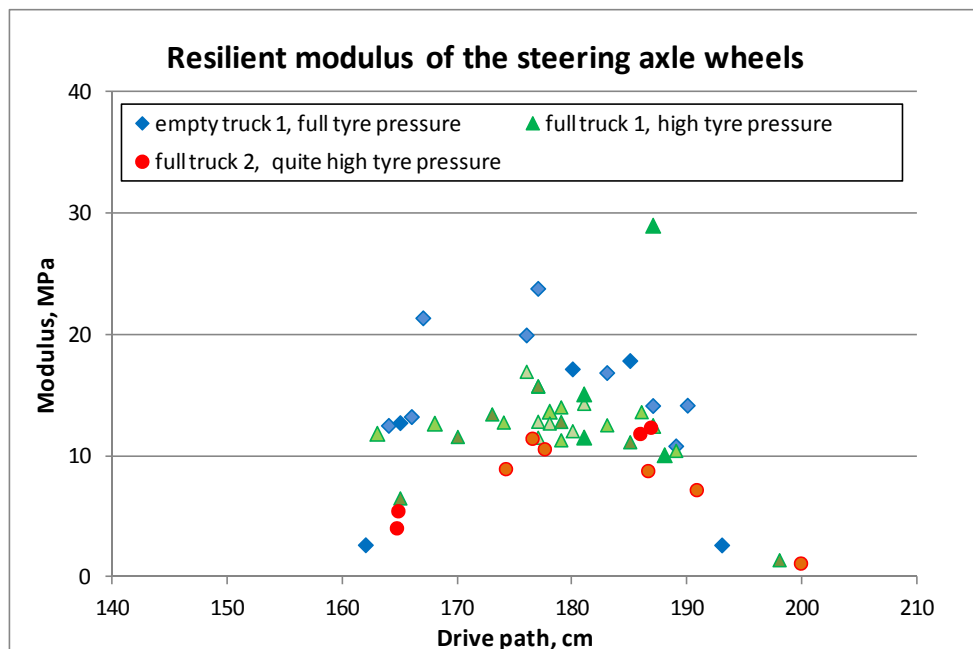


Figure 7.1 Resilient modulus of the road surface calculated from the steering axle wheels on the test site. The wheel loads were approximately 2700 kg (blue), 3300 kg (green) and 2800 kg (red).

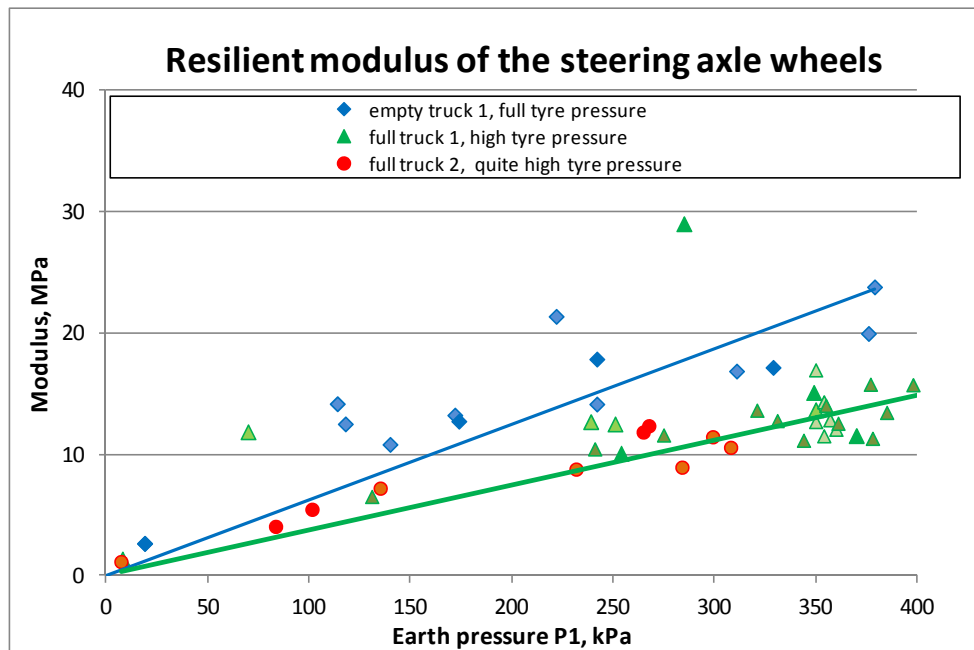


Figure 7.2 Resilient modulus of the road surface calculated from the steering axle wheels on the test site. The loading sequence was blue (empty Truck 1), green (full Truck 1) and red (full Truck 2)

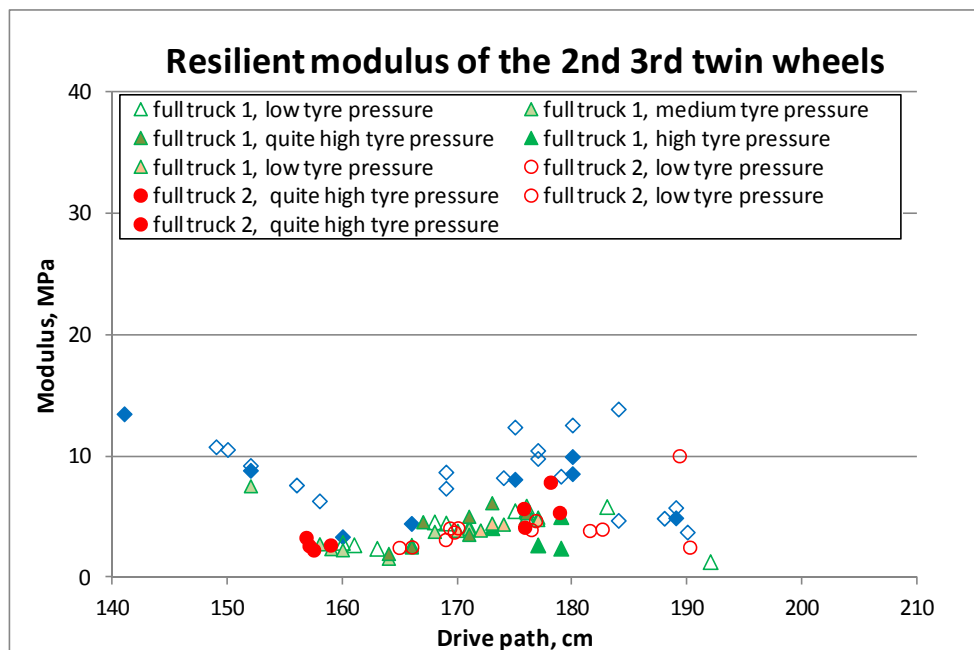


Figure 7.3 Resilient modulus of the road surface calculated from the twin wheels on the test site. Loading sequence was blue (empty Truck 1), green (full Truck 1) and red (full Truck 2).

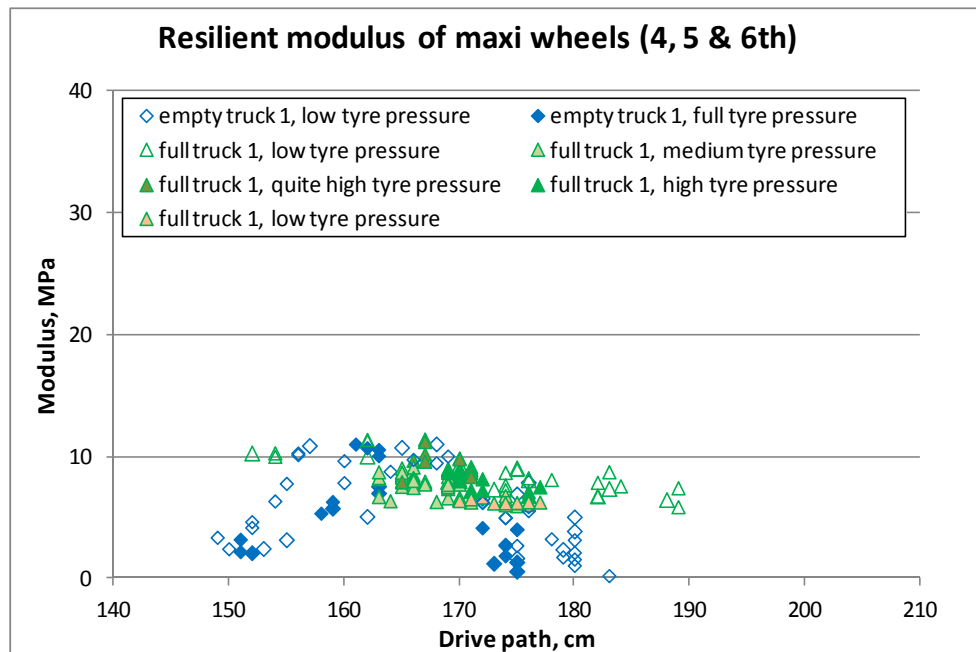


Figure 7.4 Resilient modulus of the road surface calculated from the maxi wheels on the test site. Loading sequence was blue (empty Truck 1) and green (full Truck 1)).

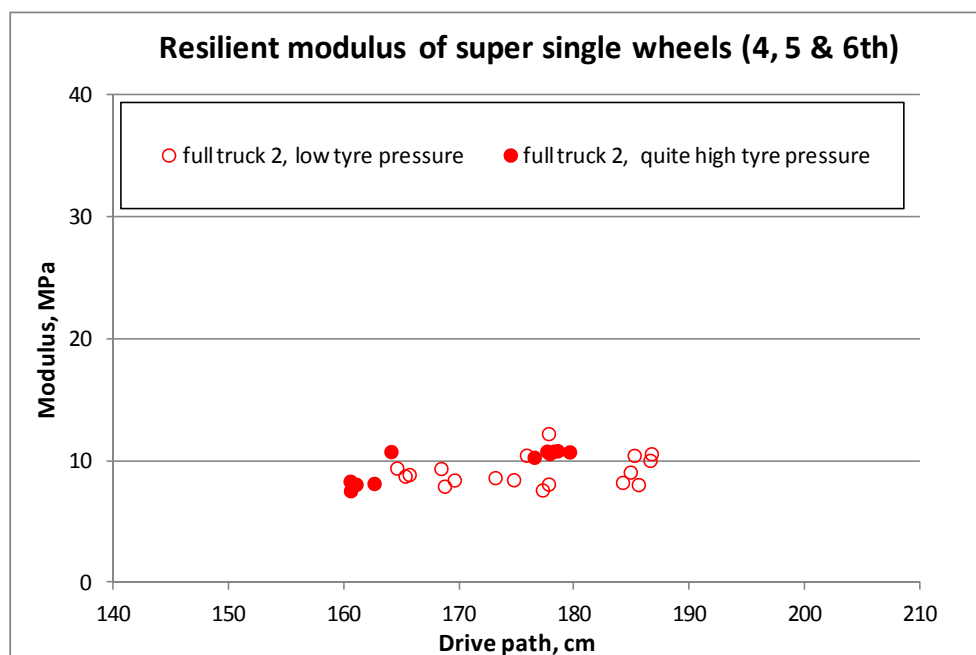


Figure 7.4 Resilient modulus of the road surface calculated from the super single wheels on the test site.

8. SUMMARY

This report summarises the results of a demonstration of CTI on a minor forest road in the Highland area of Scotland. The road was instrumented on the day prior to the testing. The road was loaded by two different forest trucks with different tyre combinations and CTI-systems (TCPS). The steering axle wheels did not have CTI fitted.

A number of conclusions can be drawn from the results of the demonstration.

The drive path had a big influence on the measured values. This was especially the case in the drive path of the twin wheels on the crown of the road. This “crowning” had an inordinate effect on the measured values for the twin wheels that they were not compared to the other wheel types within the demonstration.

Earth pressures were measured at four depths and the measured earth pressures were mainly as expected. The lower the tyre pressure was, the lower was the measured earth pressure at the depths of 67 mm and 152 mm. Changing the tyre pressure had a smaller effect at the depth of 248 mm, and at the depth of 389 mm the effect had almost vanished. The highest earth pressures were measured under the high tyre pressure single steering axle wheel near the road surface, and the highest earth pressures at the depth of 0.4 m were measured under the super single wheels. Changing the tyre pressure appeared to have had the greatest effect on the measured earth pressures with maxi wheels.

Strains were measured at one location at the depth of 35 – 155 mm, and they were big. The highest strains were measured under the steering axle wheels. The strains from the maxi and super single wheels were slightly smaller. The highest permanent strains were measured for steering axle wheel with a wheel load approximately 3300 kg. It was also noticed that the maxi wheels “pushed up” or “loosened” the layer to the same degree as the permanent deformation. Every pass of a super single wheel produced a permanent deformation at the end of the loading. At the conclusion of the demonstration the level of the road surface was measured to have settled by 10 mm to 35 mm, and the deformation between the strain gauge plates was measured as 10 mm.

The calculated resilient modulus of the road layer from the measured strains and earth pressures was low. The highest resilient modulus was below 30 MPa. It also appeared that the upper part of the road became plastic during the passes of the loaded Truck 1 with the result that the resilient modulus decreased to approximately 12 MPa during the passes of the loaded Truck 2.

When drawing conclusions from the results of the demonstration it should be remembered that the loading sequence of the trucks would also have had an effect which could not be estimated in the results. Despite this uncertainty however, based on the wheel loads and tyre pressures used in the demonstration, it seems that the steering axle wheel was the most damaging wheel near to the road surface.

ROADEX PROJECT REPORTS (1998–2012)

This report is one of a suite of reports and case studies on the management of low volume roads produced by the ROADEX project over the period 1998-2012. These reports cover a wide range of topics as below.

- Climate change adaptation
- Cost savings and benefits accruing to ROADEX technologies
- Dealing with bearing capacity problems on low volume roads constructed on peat
- Design and repair of roads suffering from spring thaw weakening
- Drainage guidelines
- Environmental guidelines & checklist
- Forest road policies
- Generation of 'snow smoke' behind heavy vehicles
- Health issues raised by poorly maintained road networks
- Managing drainage on low volume roads
- Managing peat related problems on low volume roads
- Managing permanent deformation in low volume roads
- Managing spring thaw weakening on low volume roads
- Monitoring low volume roads
- New survey techniques in drainage evaluation
- Permanent deformation, from theory to practice
- Risk analyses on low volume roads
- Road condition management of low volume roads
- Road friendly vehicles & tyre pressure control
- Road widening guidelines
- Socio-economic impacts of road conditions on low volume roads
- Structural innovations for low volume roads
- Treatment of moisture susceptible materials
- Tyre pressure control on timber haulage vehicles
- Understanding low volume pavement response to heavy traffic loading
- User perspectives on the road service level in ROADEX areas
- Vehicle and human vibration due to road condition
- Winter maintenance practice in the Northern Periphery

All of these reports, and others, are available for download free of charge from the ROADEX website at www.ROADEX.org.